Mon. Not. R. Astron. Soc. **341,** 13–32 (2003)

The Cosmic Lens All-Sky Survey – II. Gravitational lens candidate selection and follow-up

I. W. A. Browne,[1⋆] P. N. Wilkinson,[1] N. J. F. Jackson,[1] S. T. Myers,[2,4,5] C. D. Fassnacht,[4,2,8] L. V. E. Koopmans,[6,1,4] D. R. Marlow,[1,5] M. Norbury,[1] D. Rusin,[5,9] C. M. Sykes,[1] A. D. Biggs,[1,3] R. D. Blandford,[4] A. G. de Bruyn,[3] K.-H. Chae,[1] P. Helbig,[1,6] L. J. King,[7] J. P. McKean,[1] T. J. Pearson,[4] P. M. Phillips,[1] A. C. S. Readhead,[4] E. Xanthopoulos[1] and T. York[1]

[1]*University of Manchester, Jodrell Bank Observatory, Nr. Macclesfield, Cheshire SK11 9DL*
[2]*National Radio Astronomy Observatory, PO Box 0, Socorro, NM 87801, USA*
[3]*NFRA, Postbus 2, 7990 A A Dwingeloo, the Netherlands*
[4]*California Institute of Technology, Pasadena, CA 91125, USA*
[5]*Department of Physics and Astronomy University of Pennsylvania 209 S. 33rd Street Philadelphia, PA 19104, USA*
[6]*Kapteyn Astronomical Institute, Postbus 800, 9700 AA Groningen, the Netherlands*
[7]*University of Bonn, Auf dem Hügel 71, D-53121 Bonn, Germany*
[8]*STScI, 3700 San Martin Dr., Baltimore, MD 21218, USA*
[9]*Harvard-Smithsonian Center for Astrophysics, 60 Garden Street, Cambridge, MA02138, USA*

Accepted 2002 November 1. Received 2002 October 23; in original form 2002 July 10

ABSTRACT

We report the final results of the search for gravitationally lensed flat-spectrum radio sources found in the combination of CLASS (Cosmic Lens All-Sky Survey) and JVAS (Jodrell Bank VLA Astrometric Survey). VLA (Very Large Array) observations of 16 503 sources have been made, resulting in the largest sample of arcsec-scale lens systems available. Contained within the 16 503 sources is a complete sample of 11 685 sources which have two-point spectral indices between 1.4 and 5 GHz flatter than -0.5, and 5-GHz flux densities $\geqslant$30 mJy. A subset of 8958 sources form a well-defined statistical sample suitable for analysis of the lens statistics. We describe the systematic process by which 149 candidate lensed sources were picked from the statistical sample on the basis of possessing multiple compact components in the 0.2-arcsec resolution VLA maps. Candidates were followed up with 0.05-arcsec resolution MERLIN and 0.003-arcsec VLBA observations at 5 GHz and rejected as lens systems if they failed well-defined surface brightness and/or morphological tests. To illustrate the candidate elimination process, we show examples of sources representative of particular morphologies that have been ruled out by the follow-up observations. 194 additional candidates, not in the well-defined sample, were also followed up. Maps for all the candidates can be found on the World Wide Web at http://www.jb.man.ac.uk/research/gravlens/index.html. We summarize the properties of each of the 22 gravitational lens systems in JVAS/CLASS. 12 are double-image systems, nine are four-image systems and one is a six-image system. 13 constitute a statistically well-defined sample giving a point-source lensing rate of 1:690 $\pm$ 190. The interpretation of the results in terms of the properties of the lensing galaxy population and cosmological parameters will be published elsewhere.

Key words: gravitation – gravitational lensing – radio continuum: galaxies.

1 INTRODUCTION

Gravitational lens systems play a vital role in the investigation of the distribution of matter in individual galaxies and clusters (Kochanek 1993, 1995; Rusin & Ma 2001; Keeton & Madau 2001; Koopmans & Treu 2002) and in the determination of the Hubble constant, H_0 (Refsdal 1964), while statistical analyses of gravitational lens surveys can place constraints on the cosmological constant, Λ, and the matter density, Ω (e.g. Turner 1990; Fukugita et al. 1992; Carroll, Press & Turner 1992; Kochanek 1996; Falco, Kochanek &

⋆E-mail: iwb@jb.man.ac.uk

Munõz 1998; Helbig et al. 1999; Macias-Perez et al. 2000). When using lens statistics for cosmology a major concern is the statistical completeness of the samples. For example, in optical searches, lens systems can be missed if the lensing galaxy is bright compared with the lensed images or if extinction within the lens hides lensed images. Similarly, in radio searches, the existence of extended radio structure in the lensed source on the scale of the expected multiple imaging can make lensing events difficult to identify reliably. Moreover, extended radio structure makes the lensing probabilities difficult to assess as they depend both on the lens cross-section and on the intrinsic extent of the radio source being imaged. Creating a reliable and complete sample of multiple-image lens systems is not easy.

There are several ongoing or completed surveys for arcsec-scale (i.e. individual galaxy mass) gravitational lenses that have led to the discovery of multiple-image systems.[1] The largest systematic *optical* search was the *Hubble Space Telescope* (*HST*) Snapshot survey, which detected five lens systems in a sample of 502 highly luminous quasars (e.g. Bahcall et al. 1992; Maoz et al. 1993). The first large-scale *radio* survey was the MG-VLA survey (see Burke et al. 1993; Hewitt et al. 1992 for details), which also discovered five gravitational lens systems. As there was no radio-spectral index selection imposed on targets in the MG-VLA sample, some lensing events may have been missed because of the difficulty of recognizing multiply-imaged single sources in a sample in which many of the steep-spectrum sources have intrinsically complex structures (Kochanek & Lawrence 1990). However, such surveys do find examples where radio lobes are lensed into rings and this has been exploited systematically by Lehár et al. (2001).

In contrast to the MG-VLA survey, the ∼2500-source Jodrell Bank VLA Astrometric Survey (JVAS; Patnaik et al. 1992a; Browne et al. 1998; Wilkinson et al. 1998; King et al. 1999) was limited to targets with flat radio spectra ($\alpha \geqslant -0.5$ where $S \propto \nu^{\alpha}$). This approach has several advantages, as follows.

(i) Flat-spectrum radio sources have intrinsic structures dominated by a single mas radio 'core'. Thus a source found to have multiple compact components, when observed with ∼200-mas resolution, is automatically a strong lens candidate.

(ii) Higher-resolution radio mapping of lens candidates with MERLIN and VLBI is a reliable way to discriminate between intrinsic structure and multiply-imaged cores.

(iii) The probability of multiple imaging of radio cores of angular extent $\ll$ the lens Einstein radius depends only on the lens cross-section and not on the angular extent of the lensed object.

(iv) Many flat-spectrum radio sources are quasars and therefore at high redshift, thus maximizing the lensing probability.

(v) Most flat-spectrum radio sources are time-variable and, if multiply-imaged, are suitable for time-delay measurements and hence Hubble constant determination.

(vi) Any bias arising from extinction in the lensing galaxy, a major concern in assessing the completeness of optical lens searches, is eliminated.

(vii) Any radio emission from the lensing galaxy is likely to be faint and thus confusion between lens and source emission is unlikely (in contrast to the situation at optical wavelengths).

(viii) MERLIN and VLBI maps often reveal sub-structure within the lensed images on a scale $\leqslant$ the Einstein radius which provides extra constraints on the lens mass-model.

The JVAS survey led to the discovery of six lens systems, five new ones and one rediscovery; King et al. (1999). The Cosmic Lens All Sky Survey (CLASS) described here used the JVAS approach and has extended it to much larger numbers of targets and to weaker radio sources.

In order to work on a much larger sample of objects, a collaboration was initially formed between the University of Manchester group at the Jodrell Bank Observatory (JBO) and groups from the California Institute of Technology and the Netherlands (Dwingeloo and Leiden University). The CLASS team now comprises groups at JBO, the California Institute of Technology, NRAO, STScI, CfA and Dwingeloo. CLASS has concentrated on the northern hemisphere; a survey with similar goals is being pursued by others in the south (Winn et al. 2001).

The selection of targets, the VLA observations and their analysis are described in full in the companion to this paper, Myers et al. (2003), hereafter Paper I. In the present paper we concentrate on the selection of the lens candidates and the follow-up procedures; these procedures are very similar to those used for JVAS and illustrated in fig. 1 of King et al. (1999). That figure is reproduced here in slightly modified form (Fig. 1). The candidate selection, and the subsequent rejection of most of them, is discussed in some detail to validate our claim that JVAS/CLASS have produced reliable and complete lens statistics which can then be used to constrain the parameters of cosmological models (Chae 2002, hereinafter Paper III). We list the candidates which have been followed up and give the web address (http://www.jb.man.ac.uk/research/gravlens/index.html) where the MERLIN and VLBA maps can be found and examined.

2 PRIMARY SAMPLE SELECTION

Paper I gives full details of source selection and data analysis; here we give only an abbreviated account for completeness. The final CLASS complete sample was selected from the 5 GHz GB6 catalogue (Gregory et al. 1996) and the NVSS 1.4 GHz catalogue (Condon et al. 1998). Starting with GB6 we picked sources stronger than 30 mJy and looked for their counterparts in NVSS, rejecting all those with two point spectral indices steeper than −0.5. The area covered by GB6 is from declination 0° to 75°. To avoid difficulties with Galactic extinction in optical follow-up observations or confusion with extended Galactic sources such as planetary nebulae, only sources with $|b| \geqslant 10^{\circ}$ were included. A total of 11 685 GB6 sources meet these selection criteria of which all but 13 have been observed successfully.[2] The 11 685 sources include ∼2000 JVAS sources and henceforth the 'CLASS complete sample' should be understood to contain JVAS sources as a subset. Each source selected was observed

[1] See the web site of the CfA Arizona Space Telescope Lens Survey (http://cfa-www.harvard.edu/castles/) for a summary of the known multiply-imaged systems and their properties.

[2] Because the GB6 and NVSS surveys did not exist at the outset of the CLASS project, the first target sources were selected using slightly different criteria based on various combination of 87GB (Gregory & Condon 1991), the WENSS 325-MHz survey (Rengelink et al. 1997), the 365-MHz Texas survey (Douglas et al. 1996) and the NRAO 1.4-GHz survey (White & Becker 1992). This means that during the different stages of the CLASS project, a significant number of sources not in the final complete sample were observed resulting in a total of 16 503 sources being observed with the VLA (See Paper I for more details).

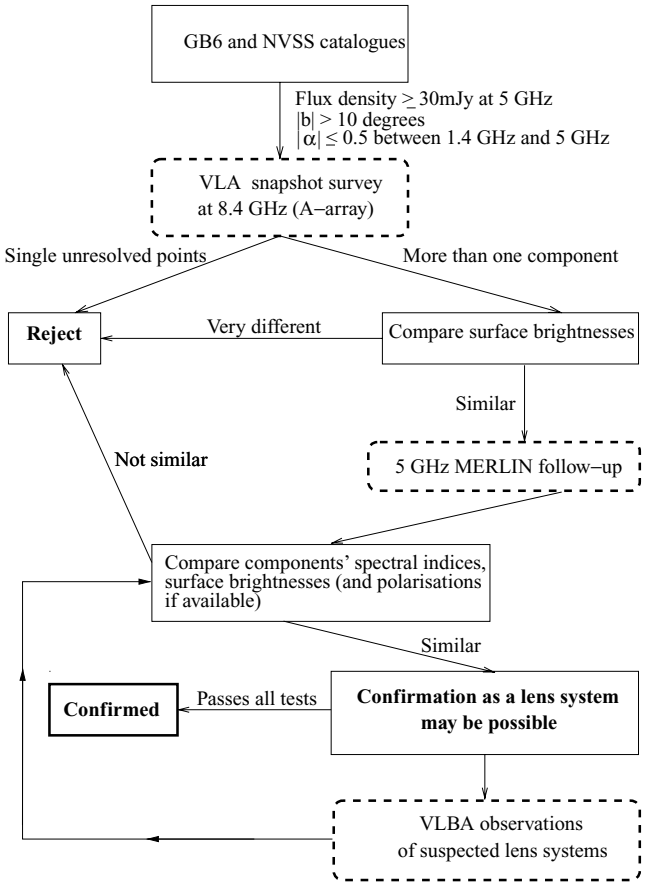

Figure 1. Flow diagram illustrating the fundamentals of the CLASS search strategy. In some individual cases extra VLA, MERLIN and VLBI observations are made where necessary. Also optical observations were attempted for those candidates that looked very promising. No candidates were ruled out on the basis of optical observations alone. This methodology is very similar to that adopted for the JVAS search (King et al. 1999).

with the VLA in its A-configuration at a frequency of 8.4 GHz, resulting in a map with a resolution of 200 mas, an rms noise level of ∼0.2 mJy and a typical dynamic range of ⩾50:1. Even though the CLASS data have been collected and reduced over a period of many years, all have been been recently re-edited, re-calibrated and re-mapped in a standard manner to ensure uniformity of data quality. Further details of the VLA observations and their analysis are given in Paper I.

3 LENS CANDIDATE SELECTION

We looked for lens systems in which there are multiple images of a compact, flat radio spectrum, core of a quasar or a radio galaxy. The crucial step in the whole survey process is the selection of candidates for higher-resolution follow-up observations. The method is then to use the higher resolution maps to distinguish multiply-imaged compact cores from more extended, non-lensed, components, the assumption being that no radio sources have more than one compact VLBI core within a few arcsec.[3] The whole candidate selection and follow-up process is illustrated in Fig. 1. The CLASS philosophy has been to follow up all objects meeting the well-defined, and cautious, selection criteria listed below, even when our initial impression from the VLA maps was that they were very unlikely to be multiply-imaged systems. It is because of this meticulous follow-up procedure that we believe that our lens sample is complete within the selection criteria. We reiterate that for our statistically complete sample we are searching only for multiply-imaged compact radio cores.[4] For candidates to be included in the systematic follow-up they must meet criteria as follows.

(i) The source must have multiple compact components each with a Gaussian diameter (FWHM) ⩽170 mas when observed with the VLA at a resolution of 200 mas (but see below).

(ii) The separation of the compact components must be ⩾300 mas; the search is currently complete out to a radius 15 arcsec from the strongest component in the map. Results of the search in the separation range 6 to 15 arcsec have already been presented by Phillips et al. (2001).

(iii) The component flux density ratio must be ⩽10:1.

(iv) The sum of the 8.4 GHz flux densities of the components must be ⩾20 mJy.

The precise criteria adopted above were dictated by the instrumental resolution and sensitivity of the VLA (see Paper I) and the need to be confident that the selection of candidates was both reliable and complete within well-defined limits. Four-image lens systems, at least those with separations ⩾0.6 arcsec, are easier to identify than two-image lens systems, as quads have more eye-catching configurations that are highly unlikely to be intrinsic to the target source. The majority of candidates have two components and these candidates required the application of our rigorous follow-up protocol to determine whether or not they were lensed images of a single source. For characteristic separations ⩽0.6 arcsec, however, quads can mimic doubles when observed with 0.2 arcsec resolution. This is illustrated by the CLASS B1555+375 system (Fig. 2; Marlow et al. 1999a) where two merging images look like a single strong and extended primary component, the third image is just detected while the fourth image revealed by MERLIN (see Fig. 10, later) is too weak to show up on the original VLA finding observations. For this reason we have taken special care and followed up all sources which resemble B1555+375. In particular, we have followed up 27 small-separation doubles in which the strongest component does not formally satisfy the angular size ⩽170 mas condition. None of these extra candidates turned out to be lens systems.

Because of the adoption of the above criteria, the effective size of the sample from which lens candidates are selected is significantly less than the 11 685 sources in the CLASS complete sample. In Table 1 we give a breakdown of the source numbers. *The 'CLASS statistical sample' which should be used in statistical analyses, contains 8958 objects.* The present paper concentrates on the follow-up of 149 candidates selected from the 8958 sources in the CLASS statistical sample. These 149 candidates are listed in Table 2. The resulting sample of 13 lens systems will be referred to as the 'statistically well-defined lens sample'. Other sources not in the complete

[3] The fact that we only have one possible candidate 'dark lens' (see Section 6.3) supports out assumption.

[4] We did not, of course, ignore obvious lens systems in which lensed extended emission dominates; e.g. 1938+666. Such objects should not, however, be used in a statistical analysis of lensing rates because the lensing probability depends both on the lens cross section and the intrinsic size of the lensed object.

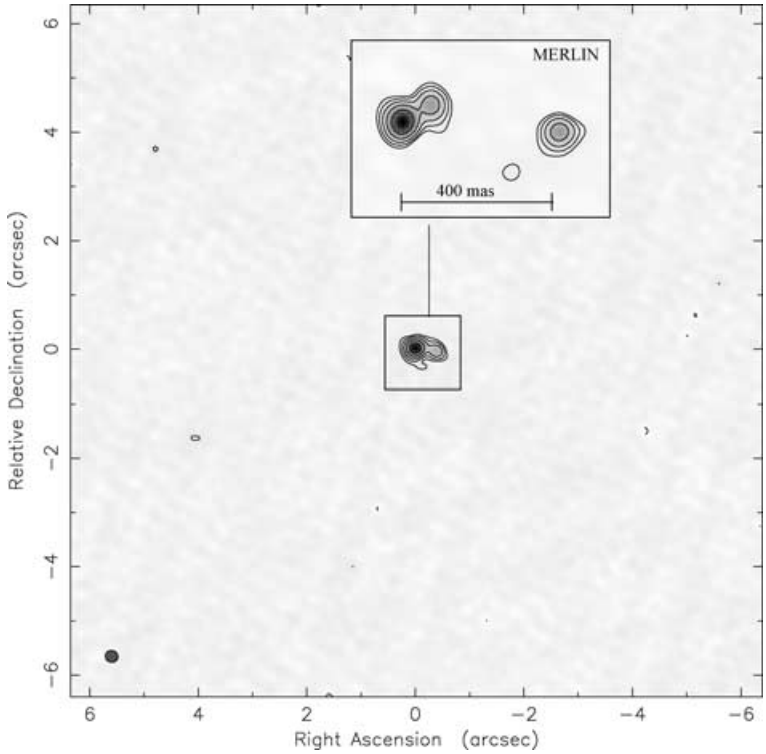

Figure 2. The VLA 8.4-GHz finding map of the compact four-image lens system CLASS B1555+375 with the higher resolution MERLIN 5-GHz map shown as an inset. Note how in the VLA map the three images merge to resemble a double source with an extended core or a core with a compact jet. The map shown in Fig. 10 shows all four images of the quad.

Table 1. Breakdown of the numbers of sources in CLASS. The 'bandwidth smeared' sources refer to a number of, mostly JVAS, observations where the VLA pointing position was more than one arcmin from the true position of the source. Under these circumstances compact components will appear artificially extended and can confuse the recognition of lens candidates.

	Number of sources
Total number of pointings	16 503
The CLASS complete sample	11 685
Failed observations	13
8.4 GHz flux density $\leqslant$20 mJy	2418
Bandwidth smeared	217
Primary component $\geqslant$170 mas	81
The CLASS statistical sample	8958

sample, but which were observed with the VLA as part of CLASS, have been treated in much the same manner for candidate selection and a further 194 candidates were followed up. Nine new lens systems have been discovered in this way (see Table 4, later). In summary, we have followed up 343 (2.1 per cent) of the 16 503 sources observed with the VLA.

Lens candidates were selected in two ways. First, by a visual inspection of the VLA maps in combination with the analysis of the automatically generated results of the modelling of each source using the CALTECH DIFFERENCE MAPPING package (DIFMAP; Shepherd 1997); the models were checked to make sure that the source met the selection criteria listed above (see Paper I for more details of the model fitting). This process was repeated several times, and by different members of the CLASS collaboration, for the entire survey. Secondly, a list of candidates was also generated automatically from the DIFMAP model-fit parameters using a figure-of-merit based on how well the model parameters conformed to the selection criteria. This second process served to cross-check the manual selection and to guard against missing candidates due to book-keeping errors. All confirmed lens systems had a figure-of-merit well above the limit that triggered follow-up observations except for the very compact four-image systems B0128+437 and B1555+375. As we have mentioned above, special precautions were taken not to miss similar systems.

The VLA discovery maps of the successful candidates are shown in Fig. 3. Some unsuccessful candidates are discussed in the next section.

4 CANDIDATE FOLLOW-UP

As illustrated in Fig. 1, we followed up candidates with stages of spatial filtering, systematically increasing the radio resolution until all candidates could be classified. As we expect lensed images of the same object to have the same surface brightness spectra and percentage polarization,[5] lens candidates were rejected if:

(i) the surface brightnesses of the putative lensed images were different by more than a (conservative) factor of $\sim$4;

[5] Multipath scattering occurring in the inter-stellar medium of the lens can change the measured surface brightness as in for example CLASS B1933+503 (Marlow et al. 1999b). However, scattering is a very strong function of observing frequency and is unlikely to be a problem at frequencies of 5 GHz or higher.

Table 2. 149 candidates for gravitationally lensed sources selected from the CLASS complete sample: the first and second columns show the J2000 IAU names and J2000 coordinates respectively. Sources marked with a ∗ are JVAS objects and have already been reported by King et al. (1999). Sources marked with a † have been reported by Phillips et al. (2001) and have component separations in the range 6 to 15 arcsec. In column 3 the instruments used for the follow-up observations are listed. Columns 4 to 7 indicate the reasons behind the rejection of candidates after the follow-up observations; the surface brightnesses (s.b.), spectral indices (s.i.) and polarizations (p.) of each candidate's components are compared in columns 4 through 6 respectively, and marked with a X where they are sufficiently dissimilar to rule out the candidate as a lens system. An X in column 7 shows that there was a morphological (m.) reason for ruling out the candidate. Notes on individual objects are given in column 8.

IAU name J2000	Coordinates J2000	Follow-up telescope	Reasons for rejection s.b.	s.i.	p.	m.	Notes
J0000+393	00 00 41.5259 +39 18 04.172	MERLIN	X		X		
J0009+400	00 09 04.1723 +40 01 46.677	MERLIN	X				
J0010+490*	00 10 02.3130 +49 01 58.584	MERLIN, VLBA	X				
J0026+351	00 26 41.7238 +35 08 42.24	MERLIN		X			Flux ratio $\geqslant$10:1
J0028+17	00 28 30.0607 +17 07 44.715	MERLIN	X			X	
J0058+141	00 58 17.8040 +14 10 48.173	MERLIN				X	
J0100+511	00 59 59.4186 +51 07 31.154	MERLIN, VLBA	X			X	$\leqslant$300 mas
J0101+115	01 01 28.2756 +11 35 31.495	MERLIN				X	$\leqslant$300 mas
J0108+198	01 09 00.8921 +19 49 55.855	MERLIN, VLBA	X				
J0111+134*	01 11 36.5675 +13 24 37.555	MERLIN	X				
J0112+379	01 12 00.2598 +37 59 31.559	MERLIN, VLBA	X				
J0138+293*	01 38 35.3186 +29 22 04.493	MERLIN	X	X			
J0152+338*	01 52 34.5718 +33 50 33.232	MERLIN		X		X	
J0210+211	02 10 59.9977 +21 10 54.641	MERLIN	X				$\leqslant$300 mas
J0212+106	02 12 42.9722 +10 41 43.369	MERLIN	X			X	
J0221+359*	02 21 05.4729 +35 56 13.819	MERLIN, VLBA					B0218+357:LENS
J0238+155	02 38 19.8898 +15 33 22.530	MERLIN	X				
J0255+026†	02 55 31.6461 +02 40 22.654	VLA	X	X			
J0307+106	03 07 58.4529 +10 35 50.835	MERLIN, VLBA					See Section 4.1.2
J0319+310*	03 19 20.7206 +31 02 11.568	MERLIN	X				
J0422+157	04 22 53.6481 +15 47 33.688	MERLIN, VLBA	X				
J0430+063	04 30 12.5330 +06 20 33.373	MERLIN	X				
J0432+639	04 32 53.9461 +63 56 40.131	VLA				X	
J0448+124	04 48 21.9905 +12 27 55.388	MERLIN, VLBA, VLA					B0445+123:LENS
J0448+098	04 48 21.7383 +09 50 51.480	MERLIN				X	
J0458+201*	04 58 29.8665 +20 11 36.115	MERLIN	X				
J0537+645	05 37 52.3575 +64 34 11.649	MERLIN	X			X	
J0552+726*	05 52 52.9690 +72 40 44.995	MERLIN	X	X			
J0558+534*	05 58 11.8134 +53 28 17.664	MERLIN	X				
J0605+627	06 05 04.4474 +62 46 53.997	MERLIN	X				
J0635+519	06 35 12.3120 +51 57 01.788	MERLIN, VLBA					B0631+519:LENS
J0641+356*	06 41 35.8456 +35 39 57.728	MERLIN	X				
J0644+465	06 44 35.3632 +46 31 17.083	MERLIN	X				
J0656+324	06 56 33.6131 +32 28 30.091	MERLIN	X				
J0704+450	07 04 50.9609 +45 02 41.623	MERLIN	X				
J0706+531	07 06 07.3296 +53 09 55.157	MERLIN, VLBA	X			X	
J0716+471	07 16 03.5799 +47 08 50.063	MERLIN, VLBA					B0712+472 LENS
J0725+195	07 25 33.0763 +19 32 14.799	MERLIN, VLBA	X				
J0732+458	07 32 19.9471 +45 50 40.150	MERLIN	X				
J0734+165	07 33 59.6960 +16 31 05.760	MERLIN	X				
J0749+578*	07 49 56.9552 +57 50 15.204	MERLIN	X				
J0753+094*	07 53 51.9407 +09 24 19.760	MERLIN	X				
J0756+449	07 56 47.5367 +44 58 55.112	MERLIN	X			X	
J0802+529	08 02 43.9915 +52 55 44.046	MERLIN, VLA	X	X			
J0803+450	08 03 40.5128 +45 00 56.937	MERLIN	X				
J0812+406	08 12 03.0283 +40 41 08.205	MERLIN	X				Flux density ratio $\geqslant$10:1
J0824+392*	08 24 55.4803 +39 16 41.982	MERLIN	X	X	X		
J0828+569	08 28 16.3028 +56 59 30.062	MERLIN	X				
J0831+524	08 31 05.4790 +52 25 21.157	MERLIN, VLBA		X			See Section 4.1.2
J0832+424*	08 32 48.4047 +42 24 59.131	MERLIN	X	X	X		
J0834+440	08 34 58.2033 +44 03 38.147	MERLIN	X				Flux density ratio $\geqslant$10:1
J0840+193	08 40 44.7018 +19 19 11.608	MERLIN	X				
J0852+052	08 52 53.5725 +05 15 15.654	MERLIN, VLBA					B0850+054:LENS
J0855+487	08 55 45.3300 +48 42 25.285	MERLIN	X				
J0856+046	08 56 17.9800 +04 38 41.550	MERLIN	X			X	
J0903+468*	09 03 03.9905 +46 51 04.133	MERLIN	X				
J0910+196	09 10 26.2070 +19 36 43.954	MERLIN	X			X	

Table 2 – *continued*

IAU name J2000	Coordinates J2000	Follow-up telescope	Reasons for rejection s.b.	s.i.	p.	m.	Notes
J0912+414	09 12 11.6157 +41 26 09.355	MERLIN	X				
J0921+716*	09 21 23.9475 +71 36 12.311	MERLIN	X	X	X		
J0930+449	09 30 14.3955 +44 57 26.425	MERLIN	X				
J0935+073	09 35 01.0733 +07 19 18.660	MERLIN, VLBA	X				See Section 4.1.2
J0936+264	09 36 14.2430 +26 24 08.100	MERLIN	X				
J0949+662*	09 49 12.1520 +66 14 59.671	MERLIN	X				
J0958+298†	09 58 58.9469 +29 48 04.179	Optical					Independent quasars (Lehár et al)
J1000+278†	10 00 29.1481 +27 52 12.168	Optical					Independent quasars (Phillips et al)
J1012+331	10 12 11.4526 +33 09 26.414	VLA		X	X		
J1034+594	10 34 34.2393 +59 24 45.846	MERLIN	X			X	
J1040+036	10 40 37.4577 +03 41 59.774	MERLIN				X	
J1124+167	11 25 00.6294 +16 44 08.145	MERLIN				X	
J1131+517	11 31 16.4545 +51 46 34.276	MERLIN, VLA	X			X	
J1132+604	11 32 58.7470 +60 29 57.151	MERLIN	X				
J1144+221	11 44 17.8365 +22 07 53.627	MERLIN	X				
J1155+196	11 55 18.3002 +19 39 42.234	MERLIN, VLBA					B1152+199:LENS
J1213+131*	12 13 32.1554 +13 07 20.556	MERLIN	X				
J1217+490	12 17 49.5808 +49 02 04.571	MERLIN	X			X	
J1236+393*	12 36 51.4519 +39 20 27.850	MERLIN	X	X	X	X	
J1240+262†	12 40 02.1435 +26 17 20.687	VLA		X			
J1246+001	12 46 02.8349 +00 07 55.144	MERLIN	X				
J1247+214	12 47 53.8655 +21 27 58.114	MERLIN, VLBA	X			X	Component separation $\leqslant$300 mas
J1252+191	12 52 27.8405 +19 10 38.182	MERLIN	X				
J1255+614	12 55 45.0142 +61 24 50.872	MERLIN	X			X	
J1312+735	13 12 48.2953 +73 35 40.634	MERLIN	X				
J1314+087	13 14 03.1904 +08 42 09.056	MERLIN	X				
J1317+344*	13 17 36.4935 +34 25 15.923	MERLIN	X	X		X	
J1326+607†	13 26 43.9112 +60 42 21.591	VLA		X			
J1329+108	13 29 01.4188 +10 53 04.799	MERLIN	X				
J1330+138	13 30 54.1248 +13 51 03.064	MERLIN	X			X	
J1401+152	14 01 35.5502 +15 13 25.638	MERLIN, VLBA					B1359+154:LENS
J1402+037	14 02 24.8410 +03 42 26.588	MERLIN	X				
J1411+006	14 11 07.8383 +00 36 07.200	MERLIN	X			X	
J1423+246	14 23 35.4922 +24 36 20.566	MERLIN	X			X	
J1424+229*	14 24 38.0544 +22 56 00.036	MERLIN, VLBA					B1422+231:LENS
J1429+541*	14 29 21.8824 +54 06 11.215	MERLIN	X	X			
J1431+731	14 31 56.2148 +73 10 40.887	MERLIN	X				
J1432+363	14 32 39.8290 +36 18 07.946	MERLIN	X				Flux density ratio $\geqslant$10:1
J1440+059*	14 40 17.9825 +05 56 34.090	MERLIN	X				
J1442+526	14 42 19.4588 +52 36 21.706	MERLIN	X			X	
J1446+144	14 46 42.3720 +14 28 01.458	VLA	X				
J1452+099	14 52 25.5265 +09 55 46.607	MERLIN, VLBA	X				
J1501+563	15 01 24.6325 +56 19 49.655	MERLIN	X			X	
J1514+509	15 14 01.4944 +50 54 29.847	MERLIN		X		X	
J1521+312*	15 21 01.2836 +31 15 37.961	MERLIN	X				Flux density ratio $\geqslant$10:1
J1528+058	15 28 44.5754 +05 52 17.402	VLBA	X				
J1540+147*	15 40 49.4620 +14 47 45.959	MERLIN	X				
J1545+529	15 45 04.9061 +52 59 25.475	MERLIN	X				
J1546+082	15 46 00.6754 +08 15 03.076	MERLIN, VLBA	X				
J1546+448	15 46 04.4211 +44 49 10.529	MERLIN	X				
J1609+655	16 09 13.9581 +65 32 28.975	MERLIN, VLBA					B1608+656:LENS
J1621+099	16 21 39.3805 +09 59 20.538	MERLIN	X				
J1625+408	16 25 10.3249 +40 53 34.339	MERLIN	X				
J1631+449	16 31 32.3744 +44 58 49.303	MERLIN, VLBA	X				
J1641+512	16 41 55.7387 +51 15 46.884	MERLIN	X			X	Flux density ratio $\geqslant$10:1
J1657+260	16 57 14.2163 +26 00 28.949	MERLIN					Component separation $\leqslant$300 mas
J1702+552	17 02 34.5570 +55 11 12.432	MERLIN, VLA				X	
J1707+232	17 07 25.4544 +23 12 21.584	MERLIN, VLBA	X				
J1708+110	17 08 25.9547 +11 04 53.091	MERLIN	X				
J1722+561	17 22 58.0083 +56 11 22.320	MERLIN	X			X	
J1724+045	17 24 52.0601 +04 35 00.390	MERLIN	X	X			
J1724+453	17 24 35.4501 +45 20 14.909	MERLIN				X	
J1726+399*	17 26 32.6614 +39 57 02.178	MERLIN	X	X	X		

Table 2 – *continued*

IAU name J2000	Coordinates J2000	Follow-up telescope	Reasons for rejection s.b.	s.i.	p.	m.	Notes
J1750+153	17 50 05.0697 +15 18 42.871	MERLIN	X				
J1802+268*	18 02 32.3014 +26 53 28.963	MERLIN	X				
J1819+307	18 19 01.4108 +30 42 23.871	MERLIN	X				
J1821+359	18 21 40.0122 +35 57 56.445	MERLIN	X				
J1835+490	18 35 21.8102 +49 04 43.612	MERLIN, VLA	X		X		
J1836+183	18 36 15.6844 +18 23 49.768	MERLIN, VLBA	X				
J1928+421	19 28 21.7712 +42 06 21.566	MERLIN				X	
J1934+504	19 34 30.8954 +50 25 23.213	MERLIN, VLBA					B1933+503:LENS
J1937+648	19 37 12.0854 +64 52 20.881	MERLIN	X				
J1947+678	19 47 36.2599 +67 50 16.928	MERLIN, VLBA	X			X	
J2030+086	20 30 04.3844 +08 39 37.536	MERLIN				X	
J2047+267	20 47 20.2885 +26 44 02.699	MERLIN, VLBA					B2045+265:LENS
J2049+127	20 49 14.4502 +12 46 42.049	MERLIN, VLBA	X				
J2049+073†	20 49 53.8362 +07 18 59.440	MERLIN			X		
J2116+024*	21 16 50.7461 +02 25 46.462	MERLIN, VLBA					B2114+022:LENS
J2125+328	21 25 18.8461 +32 52 03.907	MERLIN	X				
J2127+103	21 27 25.2300 +10 18 45.700	MERLIN				X	
J2139+190	21 39 49.5744 +19 04 34.068	MERLIN	X			X	
J2200+105*	22 00 07.9332 +10 30 07.798	MERLIN	X				
J2209+359*	22 09 45.3360 +35 56 01.017	MERLIN		X	X		
J2220+264	22 20 22.0922 +26 28 04.490	MERLIN	X				
J2241+288	22 41 14.2516 +28 52 20.119	MERLIN				X	
J2250+461	22 50 55.3802 +46 06 34.478	MERLIN, VLA			X		
J2255+434†	22 55 11.2587 +43 28 22.359	MERLIN	X	X			
J2321+454	23 21 09.0308 +45 25 42.439	VLA		X			
J2321+054	23 21 40.8044 +05 27 37.210	MERLIN, VLBA					B2319+051:LENS
J2344+278*	23 44 37.0557 +27 48 35.422	MERLIN	X	X	X		
J2355+228	23 55 27.4704 +22 53 18.093	MERLIN	X				
J2358+393*	23 58 59.8442 +39 22 28.322	MERLIN	X	X			

(ii) the structure revealed by the high resolution maps was inconsistent with lensing – for example, the radio map showed two lobes and a bridge of emission joining them, or a core plus a resolved knot in a faint underlying jet;

(iii) the spectral indices of the putative images and/or their percentage polarizations at frequencies $\geqslant$8.4 GHz were very different (see below).

We were conscious that for multiply-imaged variable sources the effects of time-delays could make the spectral indices and polarizations of the images of the same core appear different. In addition, depolarization and Faraday rotation in the interstellar medium (ISM) of the lensing galaxy could affect the polarization properties of the images differently. Thus we treated these quantities with caution when it came to rejecting candidates. Only if one component had an obviously steep spectrum, and therefore was very unlikely to be variable, did we reject a candidate on the basis of radio spectral index alone. Likewise, we disregarded percentage polarizations at frequencies $<$8.4 GHz where Faraday depolarization may be important. Even at 8.4 GHz and above we only rejected on the basis of percentage polarizations if the component polarization differed by more than a factor of 4.

The first step in the follow-up path for all candidates was a snapshot observation with MERLIN at 5 GHz. The typical time spent on each target was one hour with observations made at four or five widely spaced hour angles. These observations enabled a map to be produced with a resolution of 50 mas and a typical rms noise level of $\sim$0.2 mJy. In about 80 per cent of the cases the maps were enough to reject unambiguously the VLA-derived candidate. In the majority of these cases the extra resolution was sufficient to distinguish between the components on the grounds of different surface brightness. This was almost always in the sense that the secondary was resolved while the primary remained compact. As the secondaries are usually several times weaker than the primaries this implies a large difference in surface brightness. From the MERLIN 5 GHz results components were adjudged to be resolved if they had FWHM $\geqslant$40 mas. For some objects additional MERLIN observations at 1.7 GHz were made and for others, mostly systems with components separated by more than 6 arcsec, multi-frequency (1.4, 5, 8.4, 15 and 22 GHz) VLA observations were made (Phillips et al. 2001).

All candidates surviving the MERLIN filter were then observed with the VLBA at 5 GHz giving maps with a resolution $\sim$3 mas and an rms noise level of $\sim$0.15 mJy. The VLBA observations were again made in snapshot mode and taken at four different hour angles. By this stage all but a handful of objects could be classified unambiguously; the majority could either rejected on the basis of the criteria set out above or shown to satisfy those criteria. All but three of the remaining ambiguous candidates were finally classified on the basis of additional radio observations at different frequencies. Those objects which passed all the radio tests were regarded as 'provisionally confirmed' lens systems.

The emphasis of the follow-up then shifted from confirmation to consolidation. We sought optical and/or infrared observations to try to detect the lensing galaxy, the lensed images, and to measure their redshifts. Imaging with the *HST* and spectroscopy with the Keck Telescope proved a powerful combination. In all cases but one, that

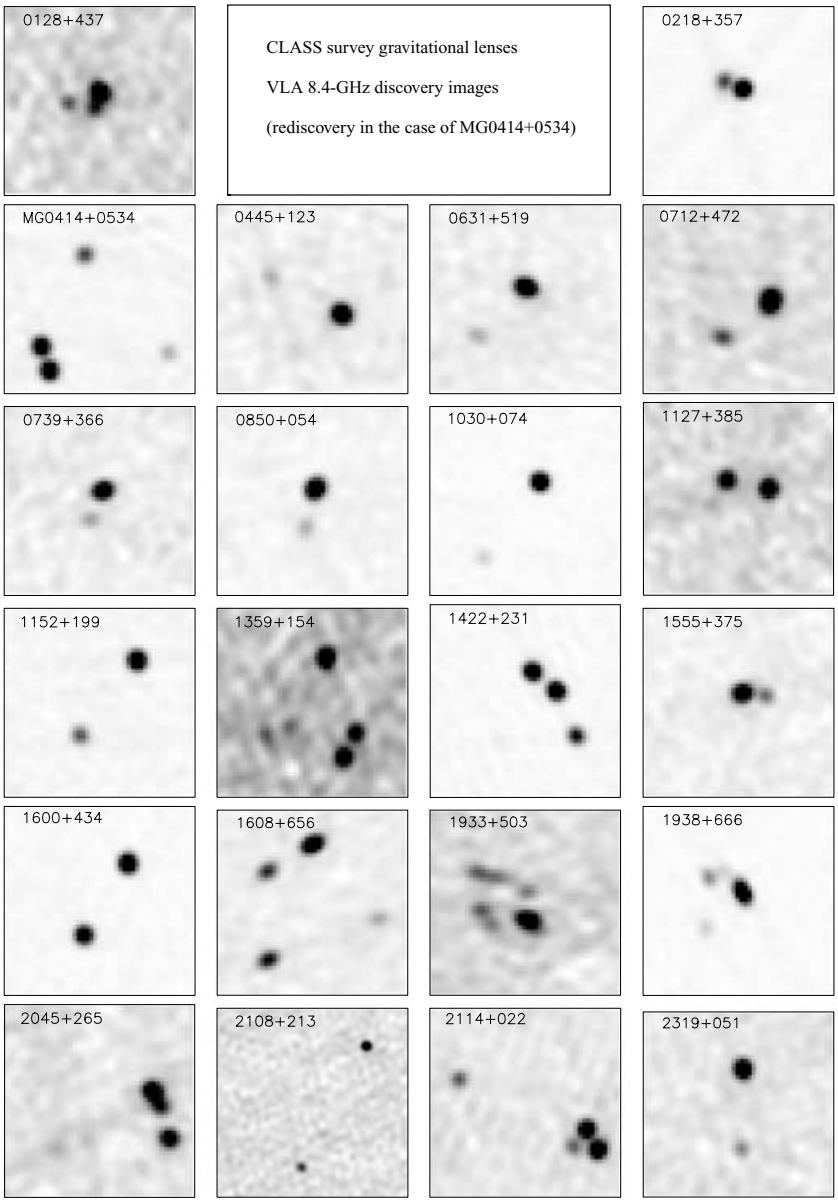

Figure 3. VLA 8.4-GHz discovery maps of the 22 successful lens candidates.

of J0831+524 (see below), these observations of the provisionally confirmed lens systems strongly supported the conclusion reached on the basis of the radio data alone. Of the 23 candidates found to have two or more mas flat-spectrum radio components in the separation range 0.3 to 6 arcsec, 22 are confirmed lens systems.

The results of the follow-up of the 149 candidates in the statistically well-defined sample are summarized in Table 2. For completeness it contains entries for those JVAS sources belonging to the sample (marked with a *) already reported by King et al. (1999). For the same reason, some of the 6 to 15 arcsec lens candidates (marked with a †) reported by Phillips et al. (2001) are included. The reasons why candidates were rejected are indicated in columns 4 to 7.

4.1 Discussion of individual candidates

In this section we illustrate the candidate follow-up procedure with some examples. We start with three simple cases in which rejection of the candidate was straightforward after only one or two sets of follow-up observations. We then discuss in some detail three of the candidates which required extensive observations and still cannot quite be ruled out with 100 per cent certainty. The majority of candidates were rejected because the surface brightnesses as revealed by the high resolution maps of the putative lensed images were different. Sometimes, but not always, the conclusion to reject on the basis of surface brightness was reinforced by the secondary structure having a jet-like morphology. Other structures which are sometimes seen are Compact Symmetric Objects (CSOs) (Wilkinson et al. 1994; Fanti et al. 1995; Readhead et al. 1996) or Medium Symmetric Objects (MSOs) (Augusto, Wilkinson & Browne 1998).

4.1.1 Examples of candidates where rejection is straightforward

J0448+098. Two well-separated and compact components of almost equal flux–density are seen in the VLA finding map.

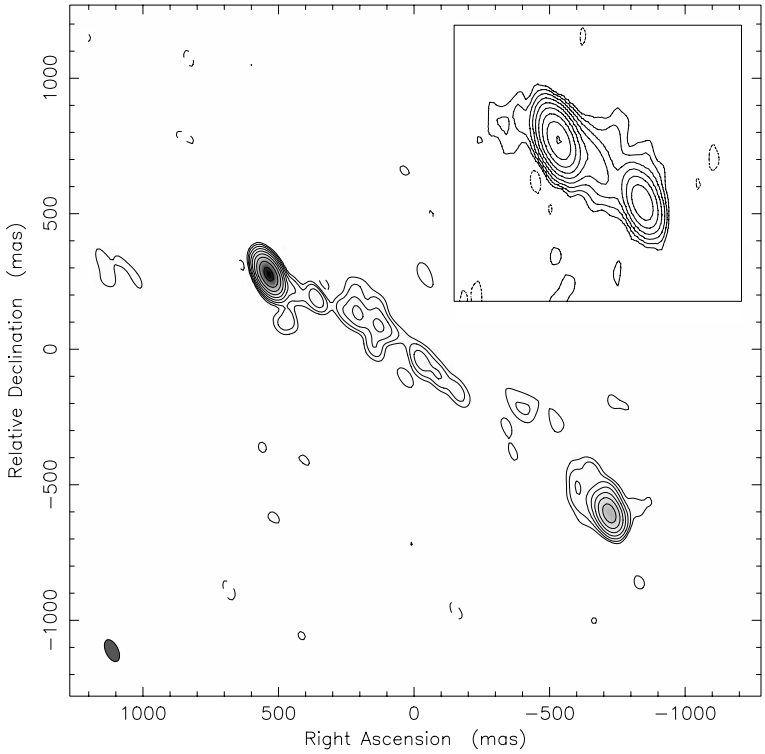

Figure 4. MERLIN 5-GHz map of the rejected lens candidate J0448+098. The VLA 8.4-GHz map is inset for comparison.

A MERLIN 5-GHz map (Fig. 4) reveals low surface brightness emission lying between the two main components, suggesting that this is an MSO or, just possibly a one-sided 3C 273-like jet. Certainly the lensing hypothesis can be rejected for this system because of the low brightness emission between the more compact outer components which could not be present if the outer components were lensed images of each other.

J0722+195. Both components of this 6:1 double are seen to be compact in a MERLIN 5-GHz map with 50 mas resolution (Fig. 5). When observed with the VLBA at mas resolution, however, the weaker secondary component was not detected and thus is of much lower surface brightness than the compact primary. The nature of this secondary component is not clear but it is not an image of the primary.

J1411+006. In the VLA 8.4-GHz finding map (inset in Fig. 6) two compact components with a flux–density ratio of 5:1 and separated by 1.4 arcsec are seen. The MERLIN 5-GHz map (Fig. 6) shows the secondary to be of lower surface brightness than the primary and, in addition, a new component is detected between the two main ones, suggesting that the structure consists of a core and knots in a faint underlying jet.

4.1.2 Examples of difficult candidates

There were just three candidates after extensive observations with MERLIN, VLBA and *HST* which could not be either ruled out nor confirmed as lensed systems with 100 per cent certainty.

J0307+106. The MERLIN 5-GHz map (Fig. 7) shows two compact radio components separated by 345 mas with a flux–density ratio of 6:1. Additional MERLIN and VLBA 1.7 and 5-GHz maps have been made and *HST* NICMOS (H) and WFPC2 (*V* and *I*) pictures have been obtained. Both radio images are dominated by compact emission even with the 3-mas resolution of the 5-GHz VLBA maps. Both components also have flat radio spectra over the frequency range 1.7 to 8.4 GHz. A relatively bright ($H = 16.7$) compact object is detected on the NICMOS picture (Fig. 7). Neither the NICMOS nor the WFPC data show any hint of the multiple components expected if there were both a lens and lensed images present. The strongest evidence against the hypothesis that J0307+106 is a lens system comes from a long-track VLBA observation at 1.7 GHz. The resulting map (Fig. 7) shows that the weaker component has a jet-like feature pointing towards the stronger component. If it were a lens system, this jet should be easily visible in the higher magnification northern image. However, it is surprising, in the non-lensing hypothesis, that both components are so compact. The only way that the lensing hypothesis could remain viable would be if the extended 'jet' emission were associated with the lensing galaxy rather than the background, lensed, radio source. Although the VLBA image makes this seems highly unlikely, we cannot rule out lensing for this source with 100 per cent certainty.

J0831+524 has been extensively followed up with both radio and optical observations and discussed in detail by Koopmans et al. (2000b). In this case, MERLIN and VLBA maps show two compact components with a separation of 2.85 arcsec. In all other cases (22 out of 23 in CLASS), the existence of two or more such components has been a reliable indicator of lensing. However, though both components have sub-mas structure, there is a hint that the weaker component is the more extended. Moreover, the radio spectral indices of the two components are significantly different. Thus the radio evidence for lensing is not entirely convincing. Optical/infrared emission is detected from the region of both radio components but with a very different flux–density ratio, 16:1, compared with the 2.8:1 observed at 8.4 GHz. We would not expect much extinction of images in a relatively symmetrical lens system with an image separation of 2.85 arcsec since both light paths will pass ∼10 kpc

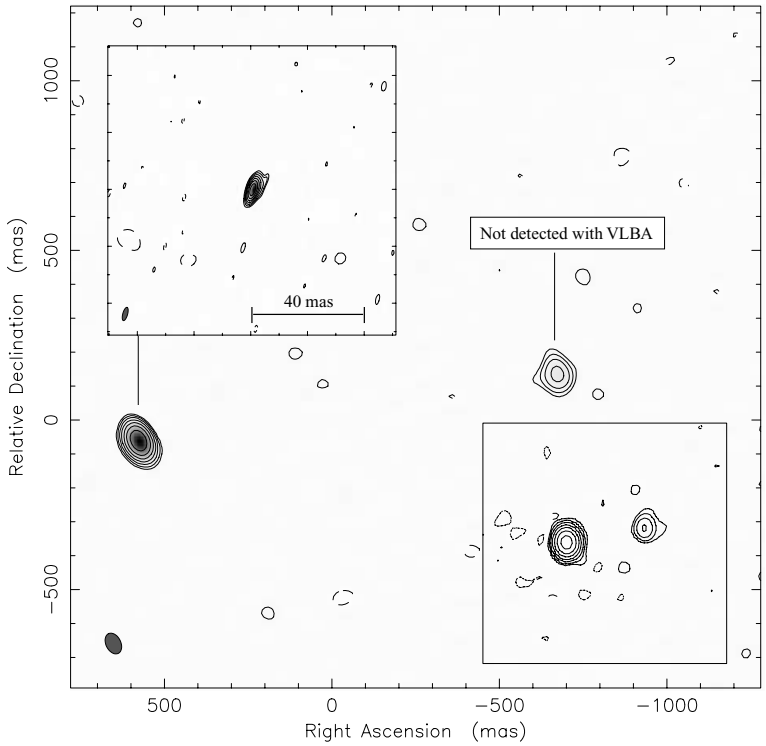

Figure 5. MERLIN 5-GHz map of the rejected lens candidate J0722+195. The VLA 8.4-GHz map is shown as an inset in the bottom right hand corner. Also shown is the VLBA 5-GHz map of the stronger, eastern, component. In the VLBA observation the weaker, western, component is not seen.

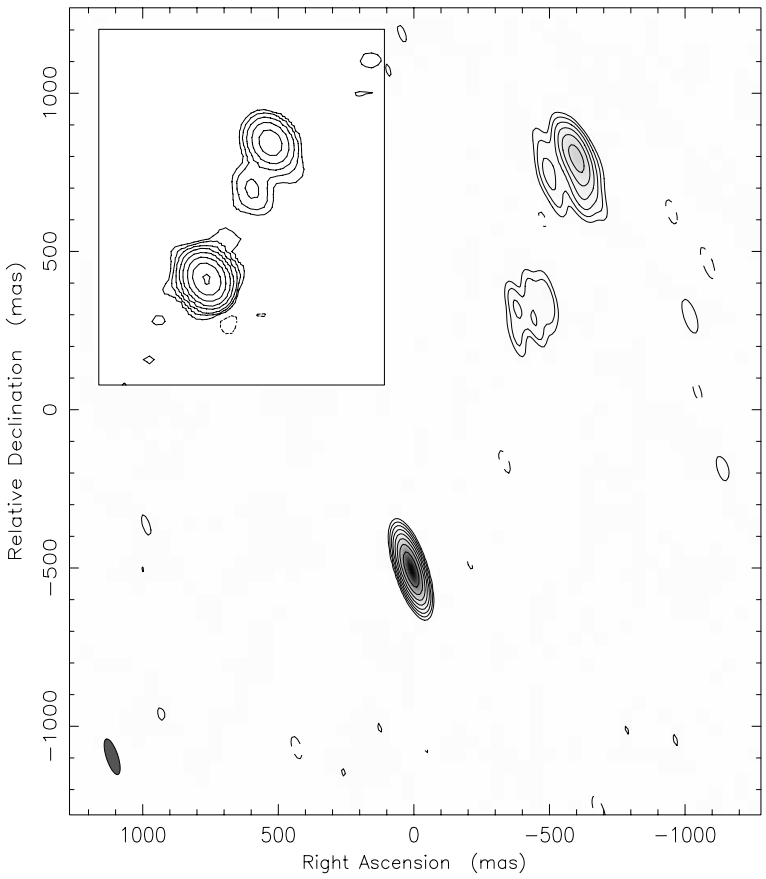

Figure 6. MERLIN 5-GHz map of the rejected lens candidate J1411+006. The 8.4-GHz VLA map is inset for comparison.

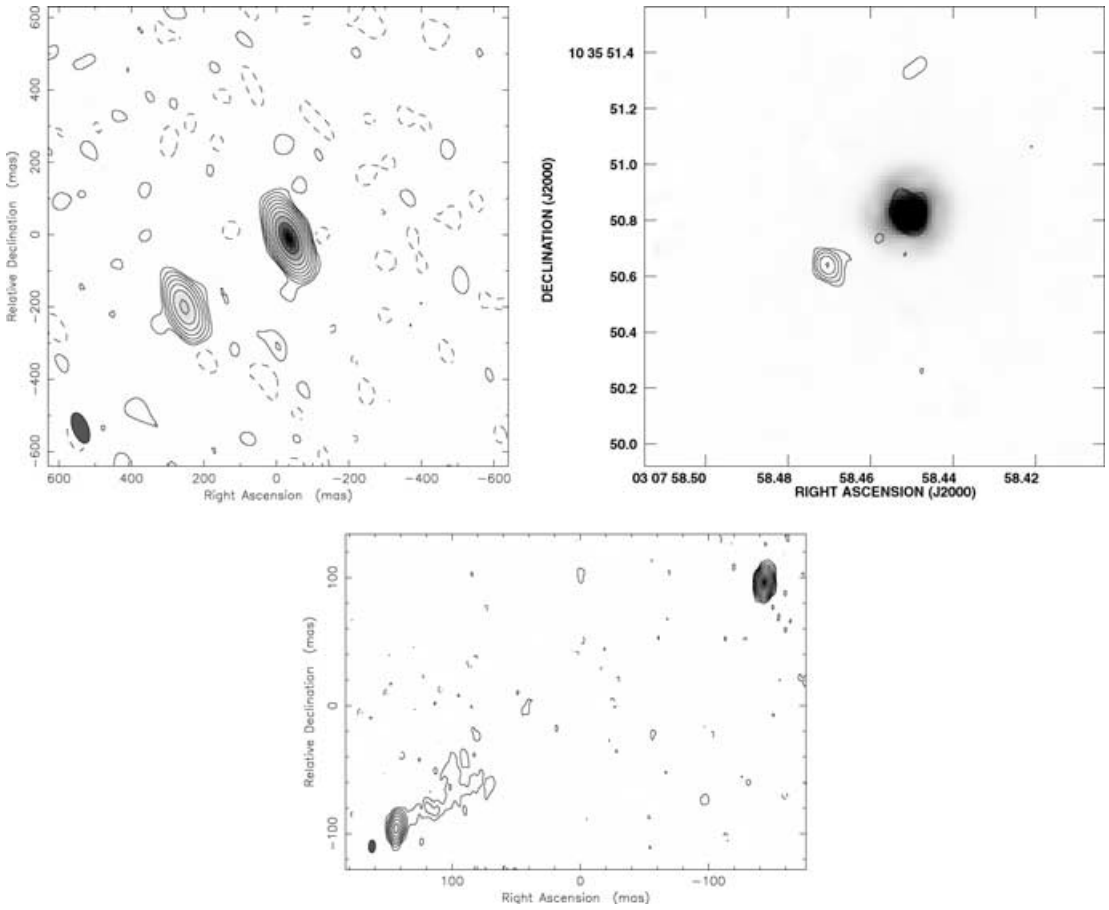

Figure 7. Radio and infrared images of J0307+106. Top row, left: MERLIN 5-GHz map of J0307+106 showing the two compact components. Top row, right: the same MERLIN map overlayed on to the *HST H*-band image of the field obtained with NICMOS. There is no evidence of extension in the NICMOS image. It should be noted that the accuracy of the registration of the NICMOS and the MERLIN pictures is ∼0.5 arcsec so it is not possible identify which, if any, of the radio components is coincident with the NICMOS object. Below: a naturally weighted 1.7 GHz VLBA map of J0307+106 restored with a 4-mas circular beam.

from the centre of the galaxy. The infrared images of the weaker component suggests that it is somewhat extended and there is no evidence for a lensing galaxy at the expected position visible in a one orbit *H*-band NICMOS picture. The accumulated evidence therefore suggests that J0831+524 is not a lens system and what we are seeing is two independent (but possibly related) radio sources. There is a redshift of 2.064 for the brighter optical counterpart but none for the weaker (Koopmans et al. 2000b). If this system has nothing to do with lensing, it is, nevertheless, highly unusual in presenting two sub-mas components with a projected separation of galactic dimensions.

J0935+073 has a component separation of 370 mas but a flux–density ratio 22.6:1; hence it would not be part of the statistically well-defined *lens* sample, even if it were a lens system. It has, nevertheless, been extensively followed up with radio and optical observations (King et al. 1999). Both components are detected in a VLBA map at 5 GHz (Fig. 8). This map shows that the strong primary component resembles a CSO with its axis pointing approximately towards the weak secondary. Optically there is an emission line galaxy, with a redshift of 0.28, at the position of the radio components (but the astrometry is not good enough to identify which component is coincident with the optical emission). There is also a detection of a 260 mJy IRAS 60-μm source near the radio position.

The primary and secondary components are almost certainly related because of their proximity and the fact that the primary points towards the secondary. In the lensing scenario, however, one would not expect the radial stretching seen in the primary. Also, the presence of a low-redshift active galactic nucleus (AGN) is naturally explained if it is the origin of the radio emission but having an AGN as the lens would have to be attributed to coincidence in the lensing hypothesis. The CSO-like radio structure of the primary fits the scenario of the whole system being associated with the AGN, though the secondary radio component does not have an obvious interpretation in this picture. While we think gravitational lensing is an unlikely explanation for J0935+073 it still cannot be completely ruled out.

5 RESULTS OF FOLLOW-UP OBSERVATIONS: GRAVITATIONAL LENS SYSTEMS

In this section we summarize the properties of the 13 gravitational lens systems contained in the statistically well-defined CLASS lens sample (i.e. satisfying the criteria set out in Section 2) and the nine additional lens systems that have been found in CLASS but which do not satisfy the criteria for inclusion in the statistically well-defined sample. In Table 3 we list the well-defined sample systems, their maximum image separation ($\Delta\theta$), image multiplicity ($N_{\rm im}$) and the

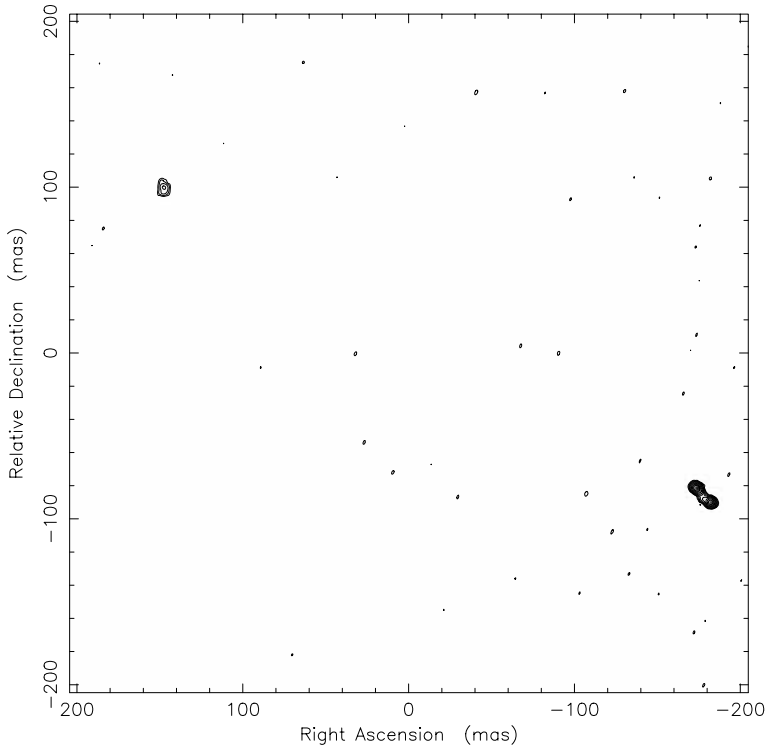

Figure 8. A naturally weighted 5-GHz VLBA map of J0935+073 restored with a 3-mas circular beam.

Table 3. Gravitational lenses in the CLASS statistically well-defined sample. The columns list the following information: column 1, B1950.0 name; columns 2 and 3, J2000.0 coordinates (in RA and Dec., respectively); column 4, the origin of the system; columns 5 and 6, source and lens redshifts respectively; column 7, the maximum image separation given in arcsec; column 8, the ratio of the flux densities of the images (for the doubles only); column 9, the number of images. The redshift references are; [1]Lawrence (1996), [2]Browne et al. (1993), [3]Jackson et al. (1998a), [4]Fassnacht & Cohen (1998), [5]Myers et al. (1999), [6]Patnaik et al. (1992b), [7]Kundić et al. (1997), [8]Fassnacht et al. (1996), [9]Myers et al. (1995), [10]Norbury, Jackson & Kerr (2003), [11]Sykes et al. (1998), [12]Fassnacht et al. (1999a), [13]Augusto et al. (2001), [14]Lubin et al. (2000), [15]Argo et al. (2003), [16]Biggs et al. (2003b).

1	2	3	4	5	6	7	8	9
B0218+357	02 21 05.4729	+35 56 13.819	JVAS	0.96[1]	0.68[2]	0.334	3.8	2
B0445+123	04 48 21.9905	+12 27 55.388	CLASS		0.557[15]	1.33	7.3	2
B0631+519	06 35 12.3120	+51 57 01.788	CLASS			1.16	6.6	2
B0712+472	07 16 03.5799	+47 08 50.063	CLASS	1.34[3]	0.41[4]	1.27	–	4
B0850+054	08 52 53.5725	+05 15 15.654	CLASS		0.59[16]	0.68	6.9	2
B1152+199	11 55 18.3002	+19 39 42.234	CLASS	1.013[5]	0.435[5]	1.56	3.0	2
B1359+154	14 01 35.5502	+15 13 25.638	CLASS	3.214[5]	–	1.65	–	6
B1422+231	14 24 38.0544	+22 56 00.036	JVAS	3.62[6]	0.34[7]	1.28	–	4
B1608+656	16 09 13.9581	+65 32 28.975	CLASS	1.39[8]	0.64[9]	2.08	–	4
B1933+503	19 34 30.8954	+50 25 23.213	CLASS	2.62[10]	0.755[11]	1.17	–	4
B2045+265	20 47 20.2885	+26 44 02.699	CLASS	1.28[12]	0.867[12]	1.86	–	4
B2114+022	21 16 50.7461	+02 25 46.462	JVAS	–	0.32/0.59[13]	2.57	3.0	2?
B2319+051	23 21 40.8044	+05 27 37.210	CLASS	–	0.624/0.588[14]	1.36	5.7	2

redshifts of the background lensed source (z_s) and lensing galaxy (z_l) where known. In Table 4 we list the nine other lens systems. Some of these are not members of the complete sample (i.e. as defined by NVSS and GB6), whereas others were followed up simply because they 'looked promising', even though they did not meet one or more of the quantitative lensing criteria set out in Section 3. Redshifts for 16 of the lensing galaxies and 11 of the lensed objects are available (see Tables 3 and 4). MERLIN 5-GHz maps of each of the 22 lens systems are shown in Figs 9 and 10. Each individual system is described briefly below.

5.1 Descriptions of the individual lens systems

CLASS B0128+437

Phillips et al. (2000) reported the discovery of this system. Infrared imaging observations made with UKIRT at 2.2 μm show the lensing galaxy and evidence for the strongest lensed image. The lensed object has a radio spectrum which is strongly peaked at ∼1 GHz and hence has a spectral index of steeper than −0.5 between 1.4 and 5 GHz, excluding it from the CLASS complete sample. VLBI

Table 4. Additional gravitational lens systems found in CLASS. The columns list the following information: column 1, B1950.0 name; columns 2 and 3, J2000.0 coordinates (in RA and Dec., respectively); column 4, the origin of the system; columns 5 and 6, source and lens redshifts respectively; column 7, the maximum image separation given in arcsec; column 8 the ratio of the flux densities of the images (for the doubles only); column 9, the number of images; column 10, the reason why each lens does not meet the criteria to be included in the statistically well-defined sample: 1 – not a member of the CLASS complete sample, 2 – the flux density ratio of the images is $\geqslant$10:1, 3 – the object is only recognized as being lensed by virtue of its extended radio emission, 4 – the sum of the image flux densities at 8.4 GHz is $\leqslant$20 mJy. The image separation is given in arcsec. References to redshifts are: [1]Lawrence, Cohen & Oke (1995), [2]Tonry & Kochanek (1999), [3]Fassnacht & Cohen (1998), [4]Tonry & Kochanek (2000), [5]Koopmans et al., in preparation.

1	2	3	4	5	6	7	8	9	10
B0128+437	01 31 13.405	43 58 13.140	CLASS			0.54	–	4	1
B0414+054	04 14 37.770	05 34 42.361	MIT/JVAS	2.62[1]	0.96[2]	2.09	–	4	1
B0739+365	07 42 51.169	36 34 43.638	CLASS	–	–	0.53	6.4	2	1
B1030+074	10 33 34.025	07 11 26.122	JVAS	1.53[3]	0.599[3]	1.56	15	2	2
B1127+385	11 30 00.099	38 12 03.091	CLASS	–	–	0.70	1.2	2	1
B1555+375	15 57 11.940	37 21 35.970	CLASS	–	–	0.43	–	4	1
B1600+434	16 01 40.500	43 16 44.000	CLASS	1.57[3]	0.415[3]	1.39	1.2	2	1
B1938+666	19 38 25.290	66 48 52.960	JVAS	–	0.878[4]	0.93	–	4	3
B2108+213	21 10 54.140	21 30 59.100	CLASS	–	0.365[5]	4.55	2.3	3?	4

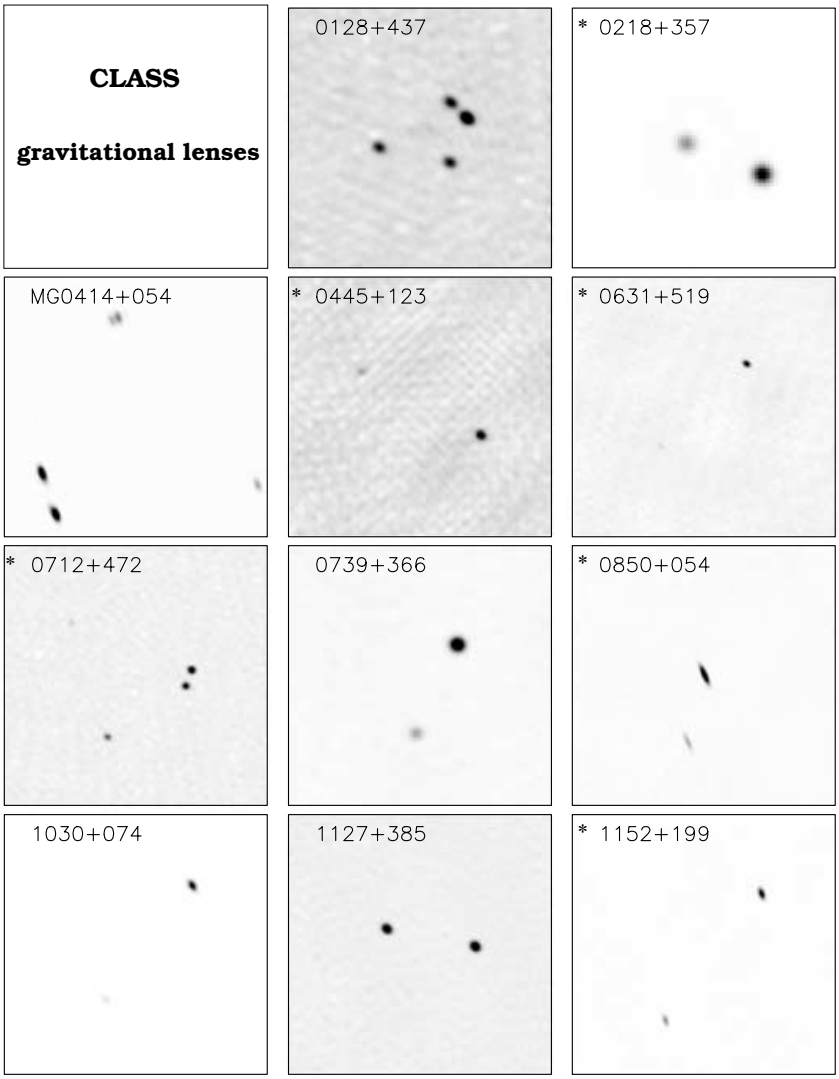

Figure 9. MERLIN 5-GHz maps of CLASS lens systems. Members of the statistically well-defined sample are marked with an asterisk.

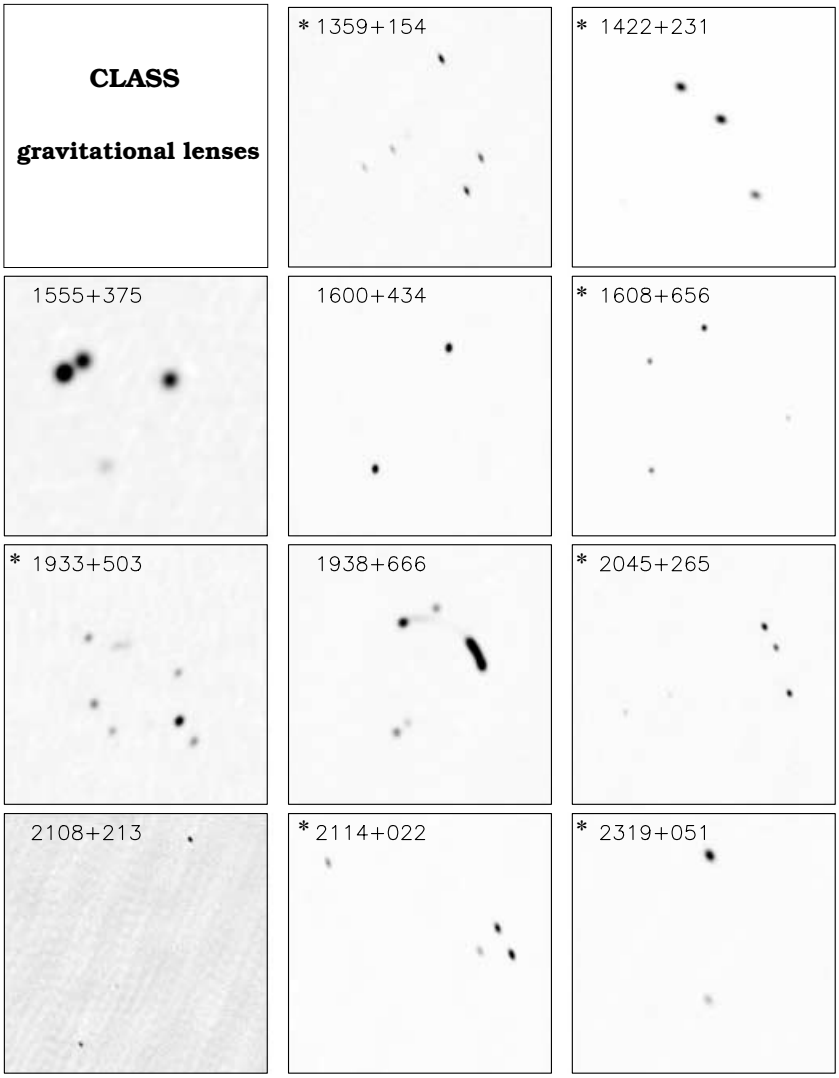

Figure 10. MERLIN 5-GHz maps of CLASS lens systems.

observations reveal a wealth of complex substructure in the lensed images. Of particular interest is that in one of the images there is no clear evidence for the compact core, which is present in all the other images. This suggests that the image may be scatter-broadened (See Section 6.2 and Biggs et al., in preparation). Barvainis & Ivison (2002) report an upper limit of 7 mJy to the 850-μm flux density.

CLASS B0218+357

Patnaik et al. (1993) reported that B0218+357 is a gravitationally lensed system. Further observations made with the VLA, MERLIN and VLBI were presented by Patnaik et al. (1993), Patnaik, Porcas & Browne (1995) and Biggs et al. (2003a) show that the lensed images contain extensive substructure. These flat-spectrum images are separated by 335 mas and the stronger is surrounded by a steep-spectrum Einstein ring of diameter 335 mas. The radio variability of the compact images has allowed a time-delay of 10.4 ± 0.4 d (95 per cent confidence) to be measured (Biggs et al. 1999; Cohen et al. 2000). The lens is a spiral galaxy which gives rise to many radio absorption lines in the spectrum of the lensed source (e.g. Menten & Reid 1996; Wiklind & Combes 1995; Carilli, Rupen & Yanny 1993). Heavy extinction in the lensing galaxy means that the stronger radio image is the fainter at optical and infrared wavelengths (Jackson, Xanthopoulos & Browne 2000).

MG 0414+0534

The four–image system B0411+054 (most often referred to by its J2000 IAU name MG0414+0534) was discovered during the MIT lens survey (Turner et al. 1989; Hewitt et al. 1992; Burke et al. 1993), and re-discovered in the course of the JVAS. It is not part of the statistically well-defined sample as its radio spectrum is too steep to meet the selection criteria. The system has been detected at 850 and 450 μm with flux densities of 25.3 and 66 mJy, respectively, by Barvainis & Ivison (2002).

CLASS B0445+123

This is one of the most recent CLASS lens systems to be discovered Argo et al. (2003). The two main images are compact on VLBA scales (∼3 mas) but there is large-scale low surface brightness structure seen in MERLIN and VLBA maps which means that it should

be possible to obtain useful observational constraints on the mass model. An optical image has been obtained with the WHT which shows an extended emission which may be a combination of the lens and lensed images. A redshift of 0.557 has been measured from a Keck spectrum obtained by McKean et al. (in preparation).

CLASS B0631+519

B0631+519 is also a recent discovery (York et al., in preparation). Like B0445+123, it has much radio structure visible on the scale of tenths of an arcsec in addition to the two main images. VLBA observations show that the most magnified image is circumferentially stretched and consists of four compact sub-components. Two galaxies, a low-redshift emission-line galaxy plus a higher redshift elliptical, have been identified spectroscopically in the system (McKean et al. in preparation); together these galaxies probably act as the lens.

CLASS B0712+472

Jackson et al. (1998b) reported the discovery of the four-image system B0712+472. The lensed object has a broad emission line, suggesting that it is a quasar, but the absolute magnitude M_v of -21.6 implies that it is a subluminous object. *HST* NICMOS images in H show the AGN host galaxy emission stretched into arcs (Jackson et al. 2000). Barvainis & Ivison (2002) measure an 850-μm flux density of 7.5 mJy. Fassnacht & Lubin (2002) have identified a foreground group of galaxies which will contribute some external shear to the mass model.

CLASS B0739+366

The GB6 5-GHz flux density of B0739+366 is 30 mJy, and therefore the source is not in the CLASS complete sample. The discovery of the system is reported in Marlow et al. (2001). *HST* WFPC2 and NICMOS pictures show the lens and the two lensed images. Barvainis & Ivison (2002) measure 850- and 450-μm flux densities of 28.8 and 71 mJy, respectively.

CLASS B0850+054

B0850+054 is a two-image system (Biggs et al. 2003b). VLBA observations at 5 GHz show that the stronger A-image is tangentially stretched over ∼20 mas and has at least five sub-components, suggesting that it is a CSO. The weaker image is radially stretched but the resolution of the existing VLBA map is not high enough to show the individual sub-components. UKIRT observations in the K band (Biggs et al., in preparation) show both the lens and the strongest lensed image. Spectroscopic observation with Keck give a redshift of 0.59 for the lensing galaxy (McKean et al., in preparation).

CLASS B1030+074

The B1030+074 system was first described by Xanthopoulos et al. (1998). The ratio of flux densities of the two images is ∼15:1 and hence it does not satisfy the criteria for it to be a member of the statistically well-defined sample. The strongest image has a well-defined jet but its counterpart in the de-magnified image is hard to see. The lensing galaxy and lensed images are seen in *HST* observations (Jackson et al. 2000). The lensing galaxy has a weak companion or an asymmetric extension. Flux density monitoring with the VLA has failed to yield a time-delay (Xanthopoulos et al., in preparation).

CLASS B1127+385

B1127+385 is not part of the CLASS complete sample because its GB6 5-GHz flux density is 29 mJy and the sample limit is 30 mJy. The discovery of this two-image system is reported by Koopmans et al. (1999). In addition to the lensed images, two lensing galaxies separated by 0.6 arcsec are seen in *HST* images. The system is detected by Barvainis & Ivison (2002) at 850 μm with a flux density of 13.9 mJy.

CLASS B1152+199

Myers et al. (1999) reported the discovery of this two-image lens system. It has been detected as an X-ray source in the northern *ROSAT* All-Sky Survey (Brinkmann et al. 1997). The weaker image is highly obscured by the lensing galaxy. *HST* pictures show the lensing galaxy which has a faint companion and VLBI observations show that both radio images consist of a compact core and a jet (Rusin et al. 2002). The system has been observed at 850 μm by Barvainis & Ivison and an upper limit of 6.4 mJy put on its flux density.

CLASS B1359+154

With six lensed images of the same source, B1359+154 is unique amongst lens systems discovered so far (Myers et al. 1999; Rusin et al. 2001a). This configuration is the result of a particularly complex deflector, which consists of three galaxies forming the core of a compact galaxy group (Rusin et al. 2000, 2001a). Barvainis & Ivison (2002) measure 850- and 450-μm flux densities of 11.5 and 39 mJy, respectively.

CLASS B1422+231

The discovery of B1422+231 as a gravitational lens system was reported by Patnaik et al. (1992b). Kundić et al. (1997) reported spectroscopy and near-infrared and optical photometry, showing that the main lensing galaxy and five nearby galaxies belong to a compact group at redshift 0.338. Observations of the mas polarization structure of the lensed images have been discussed by Patnaik et al. (1999) and a tentative time-delay derived from VLA monitoring has been determined by Patnaik & Narasimha (2001). The system has been detected in X-rays (Chartas 2000; Reeves & Reeves 2000).

CLASS B1555+375

Marlow et al. (1999a) reported the discovery of this system. B1555+375 is not part of the CLASS complete sample because its GB6 5-GHz flux density is 27 mJy and the sample limit is 30 mJy. Optical imaging with the Keck II Telescope at R band shows a faint extended object also seen in the *HST I* image. We estimate the combined emission from the lens and background source to be $R = 25$ mag. Observations at H band with the William Herschel Telescope also detected this extended object. The combined lens and background source magnitude was measured to be $H = 19$ mag. Barvainis & Ivison (2002) measure an upper limit of 6.5 mJy to the 850-μm flux density.

CLASS B1600+434

Jackson et al. (1995) reported the discovery of B1600+434. It is the clearest example of lensing by a spiral galaxy, which in this case is seen edge-on (Jaunsen & Hjorth 1997; Koopmans, de Bruyn & Jackson 1998). A radio time-delay of 47 ± 6 d between the two images has been measured by Koopmans et al. (2000a) and an optical delay of 51 ± 4 d has been reported by Burud et al. (2000). Radio microlensing has been discovered by Koopmans & de Bruyn (2000). The 5-GHz flux density of the source has been declining, causing it to drop out of the CLASS complete sample due to the change in flux density between 87GB and the more recent GB6 survey. Barvainis & Ivison (2002) measure a 850-μm flux density of 7.3 mJy.

CLASS B1608+656

B1608+656 is a four-image lens system (Myers et al. 1995) in which the core of an extended radio galaxy with a post-starburst spectrum (Fassnacht et al. 1996) is multiply-imaged (Snellen et al. 1995). *HST* observations reveal the host galaxy of the lensed object stretched into extensive arcs (Jackson, Nair & Browne 1998a). The lens seems to consist of two galaxies. Time-delays between the four radio images have been determined with VLA monitoring observations by Fassnacht et al. (1999b, 2002) (see Table 5). Barvainis & Ivison (2002) measure a 850-μm flux density of 8.1 mJy.

CLASS B1933+503

The lensed object in B1933+503 is a triple radio source (an MSO); two of the components of the triple are quadruply-imaged while the third is doubly-imaged (Sykes et al. 1998; Marlow et al. 1999b). The source shows rich mas-scale structure and, as many lines of sight through the lensing galaxy are sampled, it is an excellent system on which to test mass models (Nair 1998; Cohn et al. 2001). An attempt has been made to measure a time-delay using VLA observations, but it was unsuccessful owing to a lack of source variability (Biggs et al. 2000). Two of the lensed images are detected with NICMOS (Marlow et al. 1999b), the other two being presumed hidden as a result of extinction in the lensing galaxy. Interestingly, the same two radio images appear to suffer scatter broadening in the ISM of the lensing galaxy (Marlow et al. 1999b). Chapman et al. (1999) report the detection of the system at 850 and 450 μm with flux densities of 24 and 114 mJy, respectively, and suggest that the lensed object is a dusty quasar. A redshift of 2.62 has been recently determined for the lensed object (Norbury, Jackson & Kerr 2003).

Table 5. Gravitational lenses in the CLASS sample which have been monitored for time-delays.

Source	References	Time delay
B0218+357	Biggs et al. (1999)	B and A 10.4 ± 0.4 d
B0414+054	Moore & Hewitt (1997)	–
B1030+074	Xanthopoulos, unpublished	–
B1422+231	Patnaik & Narasimha (2001)	B and A 1.5 ± 1.4 d A and C 7.6 ± 2.5 d B and C 8.2 ± 2.0 d
B1600+434	Koopmans et al. (2000a)	B and A 47 ± 6 d
B1608+656	Fassnacht et al. (2002)	B and A 31.5 ± 3 d B and C 37 ± 3 d B and D 76 ± 3 d
B1933+503	Biggs et al. (2000)	–

CLASS B1938+666

The discovery of B1938+666 was reported by King et al. (1997). It was recognized as a lensed system by virtue of its extended arcs of radio emission and therefore is not included in the statistically well-defined sample of lens systems. The NICMOS image of the system reveals an almost perfect Einstein ring with the lensing galaxy in the centre (King et al. 1998). Barvainis & Ivison (2002) measure 850- and 450-μm flux densities of 34.6 and 126 mJy, respectively.

CLASS B2045+265

Fassnacht et al. (1999a) reported the discovery of this four-image lens system. A fifth radio component is detected but it has a different radio spectrum from the four others and is therefore likely to be radio emission from the lensing galaxy itself. The lens has an optical spectrum resembling that of an Sa galaxy (Fassnacht et al. 1999a). *HST* observations show the lensed images and the lensing galaxy. Barvainis & Ivison (2002) measure an upper limit of 3.7 mJy to the 850-μm flux density.

CLASS B2108+213

With an image separation of 4.6 arcsec, B2108+213 is the widest separation lens system in the CLASS survey (McKean et al., in preparation). Observations with the Keck Telescope show optical counterparts to the radio images as well as the main lensing galaxy at a redshift of 0.365 (Koopmans et al., in preparation). A companion galaxy within the Einstein radius is also detected and, possibly, so is a cluster of faint red objects. As well as the two main radio images, the strongest of which shows some faint extension in VLBA maps, there is a third, 1.5-mJy radio component which is either a third image or emission from the lensing galaxy. The latter interpretation is favoured, as the component seems to have an angular size of ∼50 mas in a MERLIN 5-GHz map. The sum of the 8.4-GHz flux densities of the images is <20 mJy, thus B2108+213 is not part of the statistically well-defined sample.

CLASS B2114+022

B2114+022 is the most enigmatic of the CLASS lens systems. Its discovery is reported in Augusto et al. (2001) and lens modelling is discussed in the companion paper by Chae, Mao & Augusto (2001). The radio maps show four compact components within 2.6 arcsec of each other but not in an obvious lensing configuration. Two of the components have inverted radio spectra and two have significantly steeper spectral indices. VLBI maps show that the former two components have a much lower surface brightness than the latter, supporting the view that all four components cannot be images of the same object. Two potential lensing galaxies are detected with redshifts of 0.3157 and 0.5883, but no optical emission from any of the compact radio components has been detected in either *HST* WFPC or *HST* NICMOS pictures. The most likely scenario is that two images of a distant source are being detected together with two radio components associated with the lower redshift galaxy which has a starburst spectrum. Barvainis & Ivison (2002) measure an upper limit of 4.3 mJy to the 850-μm flux density.

CLASS B2319+051

Rusin et al. (2001b) have described the lens system B2319+051. VLBA observations resolve the two images into a pair of parity-reversed sub-components separated by 20 mas in the stronger image

and 7 mas in the weaker. *HST* and ground-based optical observations reveal a primary lensing galaxy at a redshift of 0.624 and another galaxy 3.4 arcsec away with a redshift of 0.588 (Lubin et al. 2000). No optical emission has been seen from the lensed images. Barvainis & Ivison (2002) measure 850- and 450-μm flux densities of 3.9 and 40 mJy, respectively.

6 DISCUSSION

In this section we discuss some of the basic statistical properties of the CLASS lens systems. First, however, we reiterate the numbers of objects in the different CLASS subsamples, as these numbers are fundamental to the calculation of the point-source lensing rate. The CLASS complete sample of flat-spectrum radio sources, derived from GB6 and NVSS, contains 11 685 objects. However, to be on the list from which the 149 lens candidates were selected, these sources need to satisfy additional conditions (see Table 1); most importantly they need to have a total detected 8.4-GHz flux density of 20 mJy. *Hence the CLASS statistical sample used in the subsequent analysis and that of Paper III consists of 8958 objects.*

6.1 The overall lensing rate and the relative numbers of quads and doubles

Our search for multiply-imaged gravitational lens systems in a well-defined sample of flat-spectrum radio sources is complete in the specified range of parameter space; i.e. image separation between 0.3 and 15 arcsec and flux density ratio $\leqslant$10:1. There are 13 lens systems meeting these criteria amongst the 8958 sources in the well-defined parent sample. Thus the point-source lensing rate is 1 in 690 ± 190, with an error derived on the basis of Poisson statistics. The lensing rate amongst the remaining, less tightly selected, CLASS targets is similar (9 out of $\sim$5200; i.e. 1:600). This lensing rate depends on the selection criteria; we miss some systems because we restrict the image separations to be $\geqslant$0.3 arcsec and others because we require the image flux density ratios for double systems to be $\leqslant$10:1. We have made predictions of the effect of these criteria assuming the best-fitting models in flat Universe models found in Paper III. Ignoring image separations $<$300 mas will lead us to miss between 13 and 17 per cent of the systems, the exact value depending somewhat on the details of the luminosity functions adopted for the spiral and elliptical lensing galaxies. Restricting our search to separations $>$300 mas systematically selects against spiral lenses (Turner, Ostriker & Gott 1984; Augusto & Wilkinson 2001).

The percentage of double systems[6] missed due to ignoring candidates with image flux density ratios $>$10:1 is expected to be $\sim$37 per cent, the exact value depending on the distribution of ellipticities in the lensing galaxy population. This calculation assumes a slope of -2.07 for the differential number/flux density relation above 30 mJy and a slope of 1.47 below 30 mJy. We know of one CLASS system, B1030+074, with a flux density ratio $>$10:1 which has been excluded from the statistically well-defined lens sample for this reason. Because we have followed up many other high flux-ratio candidates without finding any other such lens systems, we regard 37 per cent as an upper limit to the percentage of double systems excluded for this reason.

It is also interesting to look at the relative numbers of 5-image systems (seen as quads) and of three-image systems (seen as doubles). In the statistically well-defined sample there are six quads[7] and seven doubles. If we consider all the 22 systems found in CLASS then we find 10 quads and 12 doubles. This is a higher fraction of quads than the $\sim$0.25 expected on the basis of simple models (King & Browne 1996; Kochanek 1996), and is also higher than found amongst non-CLASS lens systems. For example, amongst the non-CLASS lenses listed on the CASTLES web page (http://cfa-www.harvard.edu/castles/; Falco et al. 2001) there are nine quads and 32 doubles. However, the CLASS results are likely to be more reliable because they do not have the unknown selection biases that are suffered by the heterogeneous group of known lens systems. Rusin & Tegmark (2001) have looked at the CLASS statistics and consider a range of factors (e.g. external shear fields, mass distributions flatter than the light, shallow lensing mass profiles, finite core radii, satellite galaxies, etc.) which may increase the frequency of radio quads. They conclude that none of the mechanisms provide a compelling solution to the problem. In Paper III it is concluded that the average ellipticity of the lensing masses has to be $\geqslant$0.17 at a 95 per cent confidence level in order to fit the observed CLASS lensing statistics.

6.2 Missing doubles and multipath scattering

Could we be systematically missing double lens systems? We believe not. The only way we can suggest that this might conceivably happen is if the importance of a propagation effect such as multipath scattering occurring in the ionized ISM of lensing galaxies has been underestimated. Scattering would have the effect of increasing the angular size of an image, and hence decreasing its measured surface brightness. Thus there would be a chance of rejecting a genuine system for the reason that the measured image surface brightnesses were different. This might be a problem only for the 5-GHz VLBA observations which have a resolution of $\sim$3 mas. Multipath scattering occurring in the lensing galaxy has been invoked as a possibility in B1933+503 (Marlow et al. 1999b), in PKS 1830-211 (Guirado et al. 1999), in B2114+024 (Augusto et al. 2001) and in B0218+357 (Biggs et al. 2003a). However, B0128+437 (Biggs et al., in preparation) is the only possible case we know amongst the $\sim$60 lines of sight probed by CLASS core images in which an image surface brightness appears to have been changed enough to potentially affect our conclusions based on the 5-GHz VLBA observations. It is a quad system in which three of the images have a clearly visible compact core component, whereas the fourth does not. As it is a quad, there was no difficulty in recognizing it as a lensed system, but if one of the images of a double system had sampled the same line of sight through the lensing galaxy, it might well have been rejected. The size of a scattered image is expected to have a roughly λ^2-dependence and therefore high-frequency observations should be much less affected. We plan 15-GHz VLBA observations of $\sim$10 candidates that have been rejected on the basis of surface brightness differences in VLBA 5-GHz maps in order to eliminate any residual doubt about the completeness of the CLASS search for double-image lens systems.

6.3 Dark lenses?

Using preliminary CLASS results on 13 lensed systems, Jackson et al. (1998c) argued that the detection of the lensing galaxy with

[6] The strongest images of quad systems always have flux density ratios $\sim$ $<$3:1; Shude Mao, personal communication.

[7] Actually there are five quads plus one six-image system B1359+154 (Myers et al. 1999; Rusin et al. 2001a).

the *HST* rules out the existence of a significant number of dark lenses capable of producing image splittings of $\geqslant$1 arcsec, as suggested by Hawkins (1997). We are now in a position to update this discussion, given that there are now optical/infrared observations of sufficient quality to separate lensed images and lensing galaxies of 20 of the 22 CLASS lens systems. (For B0445+123, only ground-based imaging is currently available, and for B1555+375, existing *HST* imaging has not yet unambiguously revealed a lensing galaxy.) In all 20 cases the lensing galaxy is detected. We stress that we have not used the absence of a lensing galaxy to rule out lensing. There is just one case in which a candidate has passed all the basic radio tests and no lensing galaxy has been detected. J0831+524 (B0827+525; Koopmans et al. 2000b) was discussed in Section 4.1.2 and is the only possible dark lens candidate in CLASS. The accumulated evidence is against the lensing hypothesis, although further observations are planned. Thus the conclusion of Jackson et al. (1998c) that galaxy-mass dark lenses producing image separations in the range 0.3 to 15 arcsec are rare is reinforced by the complete CLASS results.

6.4 Image separations

A histogram of image separations for all CLASS lens systems is shown in Fig. 11. The separations peak at just over 1 arcsec, which is not very different from the predictions of Turner et al. (1984). However, it should be noted that there is evidence for multiple lensing galaxies in several of the lens systems (B1127+385, B1359+154, B1608+656, B2108+213 and B2114+022), suggesting that the characteristic image separation for lensing by a single galaxy may be $\leqslant$1 arcsec.

Only one lens system, B2108+213, has a maximum image separation $\geqslant$3 arcsec, and that is 'cluster assisted'; i.e. the lens separation is affected by the presence of several other galaxies presumed to belong to the same cluster or group as the dominant lensing galaxy. In this it resembles the first gravitational lens system to be discovered B0957+561 (Walsh, Carswell & Weymann 1979). We have searched for systems with image separations from 6 up to 15 arcsec and found none (Phillips et al. 2001). Unsuccessful searches for systems with separations $\leqslant$0.3 arcsec have been made (Augusto & Wilkinson 2001; Wilkinson et al. 2001) but with significantly fewer objects than in the CLASS sample. Nevertheless, they are sufficient to show that the lensing rate for systems $\leqslant$0.3 arcsec is lower than that for $\sim$1 arcsec with a high degree of confidence. The peak in the histogram is real.

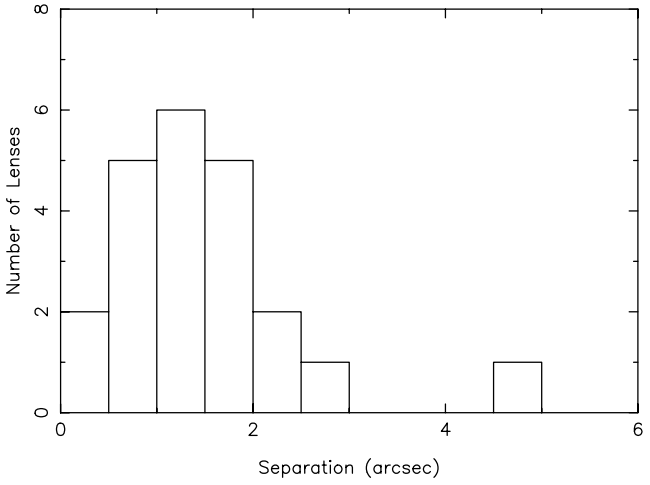

Figure 11. Separation histogram for the 22 confirmed CLASS lens systems. It should be noted that the contents of the smallest separation bin between 0 and 0.5 arcsec may be affected by the survey restriction to images separations $\leqslant$0.3 arcsec.

6.5 Time-delay and the Hubble constant

One of the aims of JVAS and CLASS was to identify lens systems suitable for time-delay measurements and Hubble constant determination. The seven systems which have been monitored systematically for time-delays are listed in Table 5. Four systems have measured time-delays, three of them (B0218+357, B1600+434 and B1608+656) with sufficient accuracy to lead to useful Hubble constant determinations in the region of $\sim$70 km s^{-1} Mpc^{-1}. Koopmans & Fassnacht (1999) summarized the various gravitational lens H_0 determinations at that time. Refined values based on analyses of new observations of B0218+357, B1600+434 and B1608+656 are likely to be available shortly.

7 CONCLUSIONS

The CLASS methodology, using high-resolution radio observations of flat-spectrum radio sources to define reliable and complete samples of gravitational lens systems, works efficiently. Many of the lens systems turn out to be suitable for time-delay measurements; time-delays have been measured for three lens systems found in the survey, and more will follow. The point-source lensing rate is 1:690 $\pm$ 190 targets. The discussion of the implications of the lensing statistics for cosmology and galaxy evolution is discussed in Paper III.

ACKNOWLEDGMENTS

We thank Shude Mao for many insightful discussions. The National Radio Astronomy Observatory is a facility of the National Science Foundation operated under cooperative agreement by Associated Universities, Incorporated. MERLIN is operated by the University of Manchester as a National Facility of the Particle Physics & Astronomy Research Council. This work was supported by the European Commission, TMR Programme, Research Network Contract ERBFMRXCT96-0034 'CERES'. This research has made use of the NASA/IPAC Extragalactic Data base (NED) which is operated by the Jet Propulsion Laboratory, California Institute of Technology, under contract with the National Aeronautics and Space Administration.

REFERENCES

Argo M. K. et al., 2003, MNRAS, 338, 957
Augusto P., Wilkinson P. N., 2001, MNRAS, 320, L40
Augusto P., Wilkinson P. N., Browne I. W. A., 1998, MNRAS, 299, 1159
Augusto P. et al., 2001, MNRAS, 326, 1007
Bahcall J. N., Maoz D., Doxsey R., Schneider D. P., Bahcall N. A., Lahav O., Yanny B., 1992, ApJ, 387, 56
Barvainis R., Ivison R., 2002, ApJ, 571, 712
Biggs A. D., Browne I. W. A., Helbig P., Koopmans L. V. E., Wilkinson P. N. Perley R. A., 1999, MNRAS, 304, 349
Biggs A. D., Xanthopoulos E., Browne I. W. A., Koopmans L. V. E., Fassnacht C. D., 2000, MNRAS, 318, 73
Biggs A. D., Wucknitz O., Porcas R. W., Browne I. W. A., Jackson N. J., Mao S., Wilkinson P. N., 2003a, MNRAS, 338, 599
Biggs A. D. et al., 2003b, MNRAS, 338, 1084
Brinkmann W. et al., 1997, A&A, 323, 739
Browne I. W. A., Patnaik A. R., Walsh D., Wilkinson P. N., 1993, MNRAS, 263, L32

Browne I. W. A., Patnaik A. R., Wilkinson P. N., Wrobel J., 1998, MNRAS, 293, 297
Burke B. F., Conner S. R., Hewitt J. N., Lehár J., 1993, in Davis R. J., Booth R. S., eds, Sub-Arcsecond Radio Astronomy. Cambridge University Press, Cambridge p. 123
Burud I. et al., 2000, ApJ, 544, 117
Carilli C. L., Rupen M. P., Yanny B., 1993, ApJ, 412, L59
Carroll S. M., Press W. H., Turner E. L., 1992, ARA&A, 30, 499
Chae K.-H., Mao S., Augusto P., 2001, MNRAS, 326, 1015
Chae K.-H. et al., 2002, Phys. Rev. Lett., 89, 1301 (Paper III)
Chapman S. C., Scott D., Lewis G. F., Borys C., Fahlman G. G., 1999, A&A, 352, 406
Chartas G., 2000, ApJ, 531, 81
Cohen A. S., Hewitt J. N., Moore C. B., Haarsma D. B., 2000, ApJ, 545, 578
Cohn J. D., Kochanek C. S., McLeod B. A., Keeton C. R., 2001, ApJ, 557, 594
Condon J. J., Cotton W. D., Greisen E. W., Yin Q. F., Perley R. A., Taylor G. B., Broderick J. J., 1998, AJ, 115, 1693
Douglas J. N., Bash F. N., Bozyan F. A., Torrence G. W., Wolfe C., 1996, AJ, 111, 1945
Falco E. E., Kochanek C. S., Munõz J. M., 1998, ApJ, 494, 47
Falco E. E. et al., 2001, in Brainerd T., Kochanek C. S., eds, ASP Conf. Ser. Vol. 237, Gravitational Lensing: Recent Progress and Future Goals. Astron. Soc. Pac., San Francisco p. 25
Fanti C., Fanti R., Dallacasa D., Schilizzi R. T., Spencer R. E., Stanghellini C., 1995, A&A, 302, 317
Fassnacht C. D., Cohen J. G., 1998, AJ, 115, 377
Fassnacht C. D., Lubin L., 2002, AJ, 123, 627
Fassnacht C. D., Womble D. S., Neugebauer G., Browne I. W. A., Readhead A. C. S., Matthews K., Pearson T. J., 1996, ApJ, 460, 103
Fassnacht C. D., Pearson T. J., Readhead A. C. S., Browne I. W. A., Koopmans L. V. E., Myers S. T., Wilkinson P. N., 1999a, ApJ, 527, 498
Fassnacht C. D. et al., 1999b, AJ, 117, 658
Fassnacht C. D., Xanthopoulos E., Koopmans L. V. E., Rusin D., 2002, ApJ, 581, 823
Fukugita M., Futamase T., Kasai M., Turner E. L., 1992, ApJ, 393, 3
Gregory P. C., Condon J. J., 1991, ApJS, 75, 1011
Gregory P. C., Scott W. K., Douglas K., Condon J. J., 1996, ApJS, 103, 427
Guirado J. C., Jones D. L., Lara L., Marcaide J. M., Preston R. A., Rao A. P., Sherwood W. A., 1999, A&A, 346, 392
Hawkins M. R. S., 1997, A&A, 328, L25
Helbig P., Marlow D., Quast R., Wilkinson P. N., Browne I. W. A., Koopmans L. V. E., 1999, A&AS, 136, 297
Hewitt J. N., Turner E. L., Lawrence C. R., Schneider D. P., Brody J. P., 1992, AJ, 104, 968
Jackson N. et al., 1995, MNRAS, 274, 25
Jackson N., Nair S., Browne I. W. A., 1998a, in Bremer M., Jackson N., Perez-Fournon I., eds, Observational Cosmology with the New Radio Surveys. Kluwer, Dordrecht
Jackson N. et al., 1998b, MNRAS, 296, 483
Jackson N., Helbig P., Browne I., Fassnacht C. D., Koopmans L., Marlow D., Wilkinson P. N., 1998c, A&A, 334, 33
Jackson N., Xanthopoulos E., Browne I. W. A., 2000, MNRAS, 311, 389
Jaunsen A. O., Hjorth J., 1997, A&A, 317, 39
Keeton C. R., Madau P., 2001, ApJ, 549, 25
King L. J., Browne I. W. A., 1996, MNRAS, 282, 67
King L. J., Browne I. W. A., Muxlow T. W. B., Narasimha D., Patnaik A. R., Porcas R. W., Wilkinson P. N., 1997, MNRAS, 289, 450
King L. J., Jackson N. J., Blandford R. D., Browne I. W. A., Fassnacht C., Marlow D. R., Nair S., Wilkinson P. N., 1998, MNRAS, 295, 41
King L. J., Browne I. W. A., Marlow D. R., Patnaik A. R., Wilkinson P. N., 1999, MNRAS, 307, 225
Kochanek C. S., 1993, ApJ, 419, 12
Kochanek C. S., 1995, ApJ, 453, 545
Kochanek C. S., 1996, ApJ, 473, 595
Kochanek C. S., Lawrence C. R., 1990, AJ, 99, 1700
Koopmans L. V. E., de Bruyn A. G., 2000, A&A, 358, 793
Koopmans L. V. E., Fassnacht C. D., 1999, ApJ, 527, 513
Koopmans L. V. E., de Bruyn A. G., Jackson N., 1998, MNRAS, 295, 534
Koopmans L. V. E., Treu T., 2002, ApJ, 568, L5
Koopmans L. V. E. et al., 1999, MNRAS, 303, 727
Koopmans L. V. E., de Bruyn A. G., Xanthopoulos E., Fassnacht C. D., 2000a, A&A, 356, 391
Koopmans L. V. E. et al., 2000b, A&A, 361, 815
Kundić T., Hogg D. W., Blandford R. D., Cohen J. G., Lubin L., Larkin J. E., 1997, AJ, 114, 2276
Lawrence C. R., 1996, in Kochanek C. S., Hewitt J. N., eds, Proc. IAU Symp. 173, Astrophysical Applications of Gravitational Lensing. Kluwer Academic Publishers, Dordrecht, p. 299
Lawrence C. R., Cohen J. G., Oke J. B., 1995, AJ, 110, 2583
Lehár J., 1992, PhD thesis, Massachusetts Inst. Technology
Lehár J., Buchalter A., McMahon R. G., Kochanek C. S., Muxlow T. W. B., 2001, ApJ, 547, 60
Lubin L. M., Fassnacht C. D., Readhead A. C. S., Blandford R. D., Kundic T., 2000, AJ, 119, 451
Macias-Perez J. F., Helbig P., Quast R., Wilkinson A., Davies R., 2000, A&A, 353, 419
Maoz D. et al., 1993, ApJ, 409, 28
Marlow D. R. et al., 1999a, AJ, 118, 645
Marlow D. R., Browne I. W. A., Jackson N., Wilkinson P. N., 1999b, MNRAS, 305, 15
Marlow D. R. et al., 2001, AJ, 121, 619
Menten K. M., Reid M. J., 1996, ApJ, 465, L99
Moore C. B., Hewitt J. N., 1997, ApJ, 491, 451
Myers S. T. et al., 1995, ApJ, 447, L5
Myers S. T. et al., 1999, AJ, 117, 2565
Myers S. T. et al., 2003, MNRAS, 341, 1 (Paper I, this issue)
Nair S., 1998, MNRAS, 301, 310
Norbury M., Jackson N. J., Kerr T., 2003, MNRAS, submitted
Patnaik A. R., Narasimha D., 2001, MNRAS, 326, 1403
Patnaik A. R., Browne I. W. A., Wilkinson P. N., Wrobel J. M., 1992a, MNRAS, 254, 655
Patnaik A. R., Browne I. W. A., Walsh D., Chaffee F. H., Foltz C. B., 1992b, MNRAS, 259, 1
Patnaik A. R., Browne I. W. A., King L. J., Muxlow T. W. B., Walsh D., Wilkinson P. N., 1993, MNRAS, 261, 435
Patnaik A. R., Porcas R. W. Browne I. W. A., 1995, MNRAS, 274, L5
Patnaik A. R., Kemball A. J., Porcas R. W., Garrett M. A., 1999, MNRAS, 307, L1
Phillips P. M. et al., 2000, MNRAS, 319, L7
Phillips P. M. et al., 2001, MNRAS, 328, 1001
Readhead A. C. S., Taylor G. B., Xu W., Pearson T. J., Wilkinson P. N., Polatidis A. G., 1996, ApJ, 460, 612
Reeves J. N., Turner M. J. L., 2000, MNRAS, 316, 234
Refsdal S., 1964, MNRAS, 128, 307
Rengelink R. B., Tang Y., de Bruyn A. G., Miley G. K., Bremer M. N., Roettgering H. J. A., Bremer M. A. R., 1997, A&AS, 124, 259
Rusin D., Ma C.-P., 2001, ApJ, 549, 33
Rusin D., Tegmark M., 2001, ApJ, 553, 709
Rusin D., Hall P. B., Nichol R. C., Marlow D. R., Richards A. M. S., Myers S. T., 2000, ApJ, 533, 89
Rusin D. et al., 2001b, AJ, 122, 591
Rusin D. et al., 2001a, ApJ, 557, 594
Rusin D., Norbury M., Biggs A. D., Marlow D. R., Jackson N. J., Browne I. W. A., Wilkinson P. N., Myers S. T., 2002, MNRAS, 330, 205
Shepherd M., 1997, in Gareth Hunt, Payne H. E., eds, ASP Conf. Ser. Vol. 125, Astronomical Data Analysis Software and Systems VI. Astron. Soc. Pac., San Francsico, p. 77
Snellen I. A. G., de Bruyn A. G., Schilizzi R. T., Miley G. K., Myers S. T., 1995, ApJ, 447, 9
Sykes C. M. et al., 1998, MNRAS, 301, 310
Tonry J. L., Kochanek C. S., 1999, AJ, 117, 2034
Tonry J. L., Kochanek C. S., 2000, AJ, 119, 1078
Turner E. L., 1990, ApJ, 365, L43
Turner E. L., Ostriker J. P., Gott J. R., III, 1984, ApJ, 284, 1

Turner E. L. et al., 1989, BAAS, 21, 718
Walsh D., Carswell R. F., Weymann R. J., 1979, Nat, 279, 381
White R. L., Becker R. H., 1992, ApJS, 79, 331
Wiklind T., Combes F., 1995, A&A, 299, 382
Wilkinson P. N., Polatidis A. G., Readhead A. C. S., Xu W., Pearson T. J., 1994, ApJ, L432
Wilkinson P. N., Browne I. W. A., Patnaik A. R., Wrobel J. M., Sorathia B., 1998, MNRAS, 300, 790
Wilkinson P. N. et al., 2001, Phys. Rev. Lett., 86, 584
Winn J. N., Hewitt J. N., Schechter P. L., 2001, in Brainerd T. G., Kochanek C. S., eds, Gravitational Lensing: Recent Progress and Future Prospects. Astron. Soc. Pac., San Francisco, p. 61
Xanthopoulos E. et al., 1998, MNRAS, 300, 649

This paper has been typeset from a TEX/LATEX file prepared by the author.